REPUBLIQUE ALGERIENNE DEMOCRATIQUE ET POPULAIRE
MINISTERE DE L'ENSEIGNEMENT SUPERIEUR ET DE LA RECHERCHE SCIENTIFIQUE

UNIVERSITE DE BLIDA
INSTITUT DES SCIENCES EXACTES
DEPARTEMENT DE PHYSIQUE

THESE

Présentée pour obtenir le diplome de Magister en Physique Fondamentale

OPTION

Astrophysique

PAR

M^lle AZI OURIDA

Sujet

THE SEASONAL EFFECT ON SOLAR NEUTRINO FLUX

Devant les membres de jury:

Président:	**M^r N.MEBARKI**	**Prof. U. Constantine**
Rapporteur:	**M^r J.MIMOUNI**	**Ph.D U.Constantine**
Examinateurs:	**M^r S.HASSANI**	**M.R CDTA**
	M^r A.ABADA	**Ph.D U.Blida**
	M^r A.AMGHAR	**Docteur INH (Boumèrdes)**

Soutenue le : 06/12/1995

REPUBLIQUE ALGERIENNE DEMOCRATIQUE ET POPULAIRE
MINISTERE DE L'ENSEIGNEMENT SUPERIEUR ET DE LA RECHERCHE SCIENTIFIQUE

UNIVERSITE DE BLIDA
INSTITUT DES SCIENCES EXACTES
DEPARTEMENT DE PHYSIQUE

THESE

Présentée pour obtenir le diplome de Magister en Physique Fondamentale

OPTION

Astrophysique

PAR

M^lle AZI OURIDA

Sujet

THE SEASONAL EFFECT ON SOLAR NEUTRINO FLUX

Devant les membres de jury:

Président:	**M^r N.MEBARKI**	**Prof. U. Constantine**
Rapporteur:	**M^r J.MIMOUNI**	**Ph.D U.Constantine**
Examinateurs:	**M^r S.HASSANI**	**M.R CDTA**
	M^r A.ABADA	**Ph.D U.Blida**
	M^r A.AMGHAR	**Docteur INH (Boumèrdes)**

Soutenue le : 06/12/1995

ABSTRACT:

The seasonal effect on solar neutrino flux is studied. Two generations of Majorana neutrino are considered. Because of the inclination of the solar axis to the ecliptic plane by an angle of $\pm\ 7^0\ 15'$ and considering the toroidal structure of the solar magnetic field in the convective zone, neutrinos crossing the sun through the equatorial plane or through regions of higher latitude, should present different amount of suppression. Indeed neutrino going through the equatorial plane were the magnetic field is thought to be zero, are not suspected to suffer from any magnetic field effect, whereas those crossing it at higher latitude, hence higher amplitude of the magnetic field, are.

However, the solar magnetic field structure is far from being well understood. One is led to consider different magnetic field configuration. A latitude dependence is also needed. To overcome such difficulty, we consider that the convective zone magnetic field is scaled by a parameter B_0 . Hence, varying B_0 is supposed to represent a latitude dependence of the magnetic field.

After a statistical analysis of the available data from Homestake and Gallex experiments, limits on neutrino particle properties are obtained, namely on the difference between the mass eigenstates and the neutrino transitional magnetic moment.

Acknowledgments

I would like to thank Dr J.Mimouni who offered me the opportunity of preparing my Master thesis with him and for the care he has shown for the completion of this thesis.

My great thanks go specially to Dr A.Abada who was always fully available to discuss with me many important points, he helped me for many times to clarify some physical ideas. His high human qualities should be mentioned.

I wonder if there is any way to let Dr Guessoum know about my acknowledgment for the encouraging attitude he has shown during the years when he was at the Institute of Physics at Blida.

Dr Boulares who is no more among us has let a large impact in the Institute of Physics of Blida University.

Thanks to Dr Ouared who has always kindly accepted to send me various papers every time I asked him for.

Thanks to Pr E..Schatzman from "l'observatoire de Meudon" who helped me to get the necessary data from neutrinos detectors and for all his suggestions.

My sincere appreciation goes to the examinators for accepting to discuss this thesis, namely Pr N.Mebarki from Constantine Insitute of Physics, Dr S.Hassani from CDTN (Algiers), Dr A.Amghar from INH (Boumerdes) and Dr A.Abada

This thesis couldn't be achieved in its final form without the good understanding of the group of the Department of Theoretical Physics of Constantine University, thanks to the professors, graduate students and to the secretary of the department.

Thanks to all the members of my family for their encouragement and their understanding. Thanks to my sister Nabila without whom the computational aspect of this work couldn't be achieved.

May my close friends find here my acknowledgments for their encouragement.

اهداء

على ذكرى ابي

الى امي عرفانا بتضحياتها

اهدي هذا العمل المتواضع الذي كانت وراء تحقيقه

CONTENTS:

"We are witnessing a true " Renaissance" of neutrino Physics".

C. Rubbia

INTRODUCTION:

Radioactive phenomena were observed since 1896, however their interpretation became available only by around 1930. The continuity of the energy spectra of electrons produced in β decay (assumed to be a two-body reaction), revealed the possibility of violation of the fundamental physical laws in such processes. Pauli postulated the existence of a massless neutral fermion (called later by Fermi), the neutrino. Fermi took into account this particle to establish the theory of β disintegration. The theory was very successful at low energies. However, the observation of the hypothetical particle has been possible only in 1956 by Cowan and Reines ($\overline{\nu}_e$) while the observation of another generation neutrino ν_μ had been possible only by 1962 [1].

Up to now, many of the neutrinos properties remain unknown although their understanding is of great importance. For instance, the neutrino is the most abundant form of matter in the universe next to radiation. A massive neutrino should certainly affect the density of the universe, which has to be compared to the critical density, to deduce about the future of the universe. Neutrino is abundantly produced in the nucleosynthesis reactions, and it plays a crucial role in the formation of heavy elements that are the basis of organic life. There are some speculation that neutrinos constitute the dark matter and that they are at the origin of the fluctuations that introduce local inhomogenity in the matter distribution needed for galaxy formation [2]. On the other hand neutrinos detection has been considered as an efficient probe of the solar interior. However, a deficit in neutrinos fluxes from various sources, atmospheric, sun, had been observed. The results of the operating experiments are in conflict with the most accurate theoretical calculations. This conflict between theory and observation is known as the solar neutrino problem. It is, for instance, a proof of the lack of precise information on neutrino properties. If the neutrino mass and magnetic moment are indeed equal to zero as it is the case in the Minimal Standard Model (MSM) of the electroweak interaction, then the problem can be considered from its astrophysical aspect. The understanding of stellar evolution seems to be closely related to that of the

neutrino physics. After the understanding of the thermonuclear origin of the energy that maintains stars in equilibrium, many efforts have been concentrated on the description of the stellar evolution. The basic equations were given by Chandrasekhar and Schwarzschild. However, there was no way to verify such models. Pontecorvo proposed the detection of solar neutrinos as a probe of the solar interior. R.Davis worked on the first experiment ,many others have been elaborated after the observation of neutrinos deficit.

Table 1

Target	Energy Source(s) (Mev)	Measured (SNU[1])	BSSM[2] (SNU)
^{37}Cl (Homestake)	≥ 0.8	2.23 ± 0.23	8.0 ± 1.0
$\upsilon + e$ Kamiokande (II and III)	≥ 7	2.7 ± 0.2(stat) ± 0.4(syst)	$5.69 \pm .43$
^{71}Ga GALLEX	≥ 0.2	77.1 ± 8.5 (stat) ± 6.9 (syst)	31.5 ± 14
^{71}Ga SAGE	≥ 0.2	58 ± 29(stat) ± 14(syst)	131.5 ± 14

The different experiments confirmed the solar neutrino problem. The Gallex experiment which had been recently calibrated confirmed that the deficit is actually a real effect (see table 1, [3])

By considering a neutrino physics beyond the MSM or other assumptions than those considered in the Standard Solar Model (SSM), this problem has to be solved following these two approaches. Many solutions have been suggested.

[1] The unit SNU is defined to be 1 capture per 10^{36} target atoms per second.
[2] Standard Solar Model which follows from the calculations of Bahcall.

The reduction of the central temperature (T_C) of the Sun, appears to be a plausible solution. It is the main idea that motivates most of the astrophysical solutions. The temperature gradient characterizing a radiative transfer is proportional to the opacity. The central temperature can be reduced by decreasing the opacity. This can be achieved by assuming a lower abundance for the heavy elements such as iron. Other models consider more terms in the equation of hydrostatic equilibrium than in the SSM. In fact in the latest case, it is only the particle pressure and radiative pressure that balance the gravitational collapse. Other forms of energy are considered in such model as the so called: Non Standard Solar Model (NSSM). The rotational energy could also minimize the thermal energy thus reducing T_C. Other models suppose the existence of "Weak Interacting Massive Particles"(WIMP) which can escape from the solar core thus opening a new channel of energy loss. NSSM are disfavored by most of the astrophysicits. Indeed, SSM provide a good description of the sun oscillations. From an other hand, neutrinos fluxes from different sources depend on the temperature in different power, $\Phi_{B^8} \sim T_C^{18}$ and $\Phi_{Be^7} \sim T_C^8$ [4], no reconciliation between the different fluxes seems to be possible.

Other possible solutions are related to neutrino physics. The different ways in which electron neutrino can be turned out into sterile neutrino are considered. Matter oscillation effect and resonant spin flip precession are the most favored. The possibility of neutrino disintegration has been ruled out by SN1987A observations. If such process was possible, no neutrino from supernova explosion would have been detected. 20 events had been registered in Kamiokande and Homestake.

Resonant matter oscillation was first introduced by Wolfenstein and then studied in the case of solar matter by Mikheyev and Smirnov after whom it is named (MSW) [5,6]. It is one of the most natural solutions, since it considers an effect that is already known to exist for the quarks, that of flavor mixing. According to this effect mass eigenstates are related to flavor states through mixing, provided that the neutrinos are not massless.

Electron neutrino, for example, will oscillate to an other flavor υ_τ or υ_μ. A second solution is based on the possibility of a non vanishing magnetic moment. It was motivated by the apparent anticorrelation between neutrino rate detected at Homestake and the eleven years solar cycle. This effect makes possible the conversion of a left handed neutrino into a right handed one, thus becoming unobservable [7,8]. The possibility of spin-matter resonance has been illustrated later see [9,10].

Our thesis deals with the study of the seasonal effect on solar neutrinos rate. By considering observational limits on this effect, we determine some limits on neutrino properties. We will consider the conjugate effect of spin-matter conversion.

The basic idea is related to the fact that the axis of the sun is not perpendicular to the plane of earth's orbit (ecliptic plane) but makes an angle of about 7°15'. In the equatorial plane of the Sun, the magnetic field is supposed to be minimal. Thus neutrinos coming through the equatorial plane will not undergo as much spin flip as those crossing the Sun at higher latitude. Because of the tilt of the solar axis, the Earth passes through the sun's equatorial plane twice a year, namely in the beginning of June and December. Therefore,during these times, the neutrinos capture rate on Earth should be higher than that during any other month. The flux in the beginning of September and March should be minimum, it corresponds to the period when the Earth is near the maximal latitudes ($\pm 7°15'$).

Unfortunately, very little is known about the solar magnetic field. Its configuration could be understood as the consequence of the dynamo effect which induces a turbulent motion of the conductive fluid of the solar matter. This motion generates a constant large scale magnetic field superposed to a fluctuate component. Its toroidal form is such that it has a minimum near the sun's equatorial plane. Homestake experiment is the only experiment which has observed the neutrinos rate time variation until now. The reason is possibly due to the difference in the energy domain of sensibility of the working detectors. It is clear that the resolution of this problem will bring more light on either the models of stellar evolution or those of neutrinos physics.

We have divided our work in five main sections. In the first section, we will give a brief summary of the (MSM), and will see how to associate a mass and a magnetic moment to the neutrino, by considering it as a Majorana or a Dirac particle. In the second chapter, we will discuss the main two effects of neutrino transmutation, resonant matter conversion (RMC) and the resonant spin flip precession (RSFP). The third section deals with the solar structure, we will discuss the main reactions that produce neutrinos, and then describe the basis of stellar structure. SSM will be dealt with as well as some of NSSM. We discuss in the section that follows the fourth one the solar magnetic field to introduce the seasonal effect, and give details on the numerical procedure. In the last chapter, we will go into computing the seasonal effect. We will determine, for different magnetic field profiles, the domain of the magnetic moment and the mass difference squared between υ_e and υ_μ for example, that could make the seasonal effect observable. The main properties of the existing and the projected neutrinos detectors has been relegated to an appendix.

We shall finally conclude by summarizing our results and discussing future perspectives....

CHAPTER 1

NEUTRINO PHYSICS:

1.1: MINIMAL STANDARD MODEL OF THE ELECTRO-WEAK INTERACTION:

It is the present day wisdom in field theory that interactions are generated from local gauge symmetries while the masses of the particles are the results of a spontaneous symmetry breaking (SSB) of a scalar field, the so called Higgs.

The standard model for the electro-weak interaction is based on the gauge group SU(2)⊗U(1) [11]. The production of the doublets (e, ν_e), (μ, ν_μ) and (τ, ν_τ) motivated the choice of the SU(2) symmetry group. Such a symmetry will introduce the gauge bosons coupled to the weak isospin currents:

$$J_\mu^+ = \overline{\Psi}_L \gamma_\mu \sigma_+ \Psi_L$$
$$J_\mu^- = \overline{\Psi}_L \gamma_\mu \sigma_- \Psi_L$$

where $\Psi_L \equiv \begin{pmatrix} \nu \\ \ell \end{pmatrix}_L$ (1.1)

and $\sigma_\pm = \frac{1}{2}(\sigma_1 \pm i\sigma_2)$; σ_i being the Pauli matrices.

The neutral current would be identified with : $J_\mu^3 = \overline{\Psi}_L \gamma_\mu \sigma^3 \Psi_L$. However, because of the neutral current parity conservation, it seems necessary to complete the structure of the symmetry by the U(1) group and add a weak hypercharge current J_μ^Y. The three generators Q, σ_3 , Y are such that:

$$Q = \sigma^3 + \frac{1}{2} Y$$
$$\text{or} \quad J_\mu^{em} = J_\mu^3 + \frac{1}{2} J_\mu^Y \tag{1.2}$$

The masses of the propagators must follow from Higgs mechanism. In fact direct terms $(\overline{\Psi}\Psi)$ violate the SU(2)⊗U(1) symmetry. According to this mechanism a spontaneous breaking of a local symmetry will break down the mass degeneracy.

1.1.1 : Mass Spectra:

a- *Gauge bosons masses*:

Consider the following Lagrangian, restricted to the (ν_e, e) doublet:

$$L_1 = \overline{\Psi}_L \gamma_\mu \left(i\partial^\mu - \frac{g}{2} \vec{\sigma}.\vec{W}^\mu + \frac{g'}{2} B^\mu \right) \Psi_L + \bar{e}_R \gamma_\mu \left(i\gamma^\mu + g' B^\mu \right) e_R$$
$$- \frac{1}{4} \vec{W}_{\mu\nu} \vec{W}^{\mu\nu} - \frac{1}{4} B_{\mu\nu} B^{\mu\nu} \tag{1.3}$$

where the first term represent the weak isospin current coupled to the three vector W^μ ,introduced to preserve the invariance of the Lagrangian under the gauge symmetry. The second is the weak hypercharge current coupled to the vector B^μ.
The term in L_1 that leads to the boson's masses is [11]:

$$\left[\left(-ig \frac{\vec{\sigma}}{2} \cdot \vec{W}_\mu - i \frac{g'}{2} B_\mu \right) \Phi \right]^+ \left[\left(-ig \frac{\vec{\sigma}}{2} \cdot \vec{W}^\mu - i \frac{g'}{2} B^\mu \right) \Phi \right] =$$
$$\frac{1}{2} \left(\frac{gv}{2} \right)^2 \left(\vec{W}_\mu^{+^2} + \vec{W}_\mu^{-^2} \right) + \frac{v^2}{8} \left(W^{3\mu}, B^\mu \right) G \begin{pmatrix} W^{3\mu} \\ B^\mu \end{pmatrix} + \text{terms}(h^2) \tag{1.4}$$

where $W^{\pm} = \left(W^1 \mp i\, W^2\right)/\sqrt{2}$ should represent the observed charged bosons

$\Phi \equiv \frac{1}{\sqrt{2}}\begin{pmatrix} 0 \\ v + h \end{pmatrix}$ is the chosen fundamental state,

$$G = \begin{pmatrix} g^2 & gg' \\ -gg' & g'^2 \end{pmatrix} \tag{1.5}$$

g and g' are the coupling constants.

The mass eigenstates follow from the diagonalization of G.

$$\begin{aligned} A_\mu &= \frac{g B_\mu + g' W_\mu^3}{\sqrt{g^2 + g'^2}} \\ Z_\mu &= \frac{g W_\mu^3 - g' B_\mu}{\sqrt{g^2 + g'^2}} \end{aligned} \tag{1.6}$$

$$\text{with} \quad m_{A_\mu} = 0, \quad m_{Z_\mu} = \frac{1}{2} v \sqrt{g^2 + g'^2}, \quad m_{W^\pm} = \frac{g\, v}{2}$$

Z_μ should represent the observed neutral boson, A_μ represents the photon.

The diagonalizing angle θ_W is given by:

$$\begin{aligned} \cos\theta_w &= \frac{m_w}{m_z} = \frac{g}{\sqrt{g^2 + g'^2}} \\ \begin{pmatrix} A_\mu \\ Z_\mu \end{pmatrix} &= \begin{pmatrix} \cos\theta_w & \sin\theta_w \\ -\sin\theta_w & \cos\theta_w \end{pmatrix} \begin{pmatrix} B_\mu \\ W_\mu^3 \end{pmatrix} \end{aligned} \tag{1.7}$$

The success of the MSM was in the detection of the gauge bosons in the expected range of energy.

b-*Neutrino mass:*

The MSM does not incorporate the right handed component of the neutrino. Thus it is considered to be massless. On the other hand, we shall see, no Majorana mass term is allowed with in this framework.

c-*Electron mass:*

Let us introduce the following term in the Lagrangian L_1:

$$L_2 = -G_e\left[\left(\bar{\nu}_e\,,\,\bar{e}\right)_L\begin{pmatrix}\phi^+\\ \phi^0\end{pmatrix} e_R + \bar{e}_R\begin{pmatrix}\phi^-\\ \phi^0\end{pmatrix}^+\begin{pmatrix}\nu_e\\ e\end{pmatrix}_L\right] \tag{1.8}$$

by choosing the fundamental state to be $:\phi \equiv \frac{1}{\sqrt{2}}\begin{pmatrix}0\\ v+h\end{pmatrix}$, one can deduce the electron mass to be : $m_e = \frac{G_e\, v}{\sqrt{2}}$.

d- *Case of a massive doublet:*

Consider the quarks doublet (u, d). An other Higgs doublet has to be considered, that is $\begin{pmatrix}\phi^0\\ \phi^-\end{pmatrix}$, the choice of the fundamental state of ϕ will break the symmetry of the Lagrangian to lead to the following mass term:

$$L_3 = -G_d\left(\bar{u},\bar{d}\right)_L\begin{pmatrix}\phi^+\\ \phi^-\end{pmatrix} d_R - G_u\left(\bar{u},\bar{d}\right)_L\begin{pmatrix}\phi^0\\ \phi^-\end{pmatrix} u_R + h.c \tag{1.9}$$

hence, $m_{d,u} = \frac{G_{d,u}\, v}{\sqrt{2}}$

e- *Higgs particle mass:*

The Higgs potential $:V(\phi) = \mu^2\,\phi^+\phi + \lambda\left(\phi^+\phi\right)^2, \lambda > 0 \quad , \mu^2 < 0$ (1.10)

together with the following choice of the fundamental state, $\phi = \frac{1}{\sqrt{2}}\begin{pmatrix}0\\ v+h\end{pmatrix}$, lead to the mass associated with the Higgs particle, $m_h = v\sqrt{2\,\lambda}$.

I- 2 - NEUTRINO MASS BEYOND THE MINIMAL STANDARD MODEL:

I-2-1 Limits on neutrino mass:

The principal motivation for massive neutrinos came from astrophysics and cosmology. Indeed, the rotation curves for stars of a given galaxy i.e. the plots of their speeds against their distance from the galaxy center, show a constant velocity in regions where stars density is the lowest (far from the center). By measuring the mass to light ratio, we deduce that the bulk of matter is dark. Neutrinos could in fact contribute to the hidden matter. Massive neutrinos can be extremely important for cosmology as well. Standard cosmological big bang model predicts the existence of a background neutrinos all over the universe. The number density of such background is about 8 orders of magnitude larger than the average number density of baryons. Hence even if neutrinos have a mass of about 10ev, they can contribute by a huge amount to the energy density of the universe and thus affect it evolution as a whole.

All existing data are not sufficiently precise to rules out the possibility of massless neutrinos [12]. Limits on the antineutrino mass comes from the studies of the tritium decay. The best upper limit is:

$$m_{\bar{\nu}_e} \leq 4.5 \text{ ev } (95\% \text{ CL})$$

The measure of muon momentum in π^+ decays at rest gives the limit:

$$m_{\nu_\mu} \leq 160 \text{ ev } (90\% \text{ CL})$$

Decays such as $\tau^- \rightarrow \nu_\tau + (5 \text{ or more hadrons})$ are used to extract the upper limit on ν_τ mass:

$$m_{\nu_\tau} \leq 29 \text{ Mev } (95\% \text{ CL})$$

I-2-2 Mass generation:

Theoretically one can construct neutrino mass by considering it as a Majorana or a Dirac particle. Before going further and discuss the theoretical generation of neutrino mass, let us focus on the characteristics of Majorana and Dirac particles [2,13,14,15,16].

The solution of the well known Dirac equation describing the evolution of a free relativistic fermion is given by a quadrispinor field :

$$\Psi_D(x) = \int \frac{d^3p}{(2\pi)^{3/2}} \sum_s \left\{ b_s(p) u_s(p) e^{-ipx} + d_s^+(p) v_s(p) e^{ipx} \right\} \qquad (1.11)$$

where b' and d' are the operators of creation of the particle and the antiparticle respectively.

For massless fermions, Pauli matrices are sufficient to define solutions of Dirac equation. Weyl representation is the most appropriate for such fields. Because neutral particles could be identified with their corresponding antiparticles, another description is possible, that is Majorana representation. In this case, the creation operator of the particle is just proportional to that of the antiparticle.A Majorana field satisfies the Dirac equation together with the Majorana condition:

$$C \overline{\Psi}_M^T(x) = \lambda \Psi_M(x) \qquad (1.12)$$

where C is the charge conjugation matrix satisfying the conditions:

$$C \gamma_\alpha^T C^{-1} = -\gamma_\alpha \ , C^+ C = 1 \ , \ C^T = -C \qquad (1.13)$$

hence,

$$\Psi_M(x) = \int \frac{d^3p}{(2\pi)^{3/2}} \sum_s \{ b_s(p) u_s(p) e^{-ipx} + \lambda b_s^+(p)\, u_s(-p) e^{ipx} \} \qquad (1.14)$$

where λ is a phase factor.

In the chiral representation[1], ν_L can be written in terms of the two-component spinor field φ: $\nu_L = \begin{pmatrix} \varphi \\ 0 \end{pmatrix}$, therefore, a Majorana neutrino is given by:

$$\nu_M = \nu_L + \nu_L^C = \begin{pmatrix} \varphi \\ -i\sigma^2 \varphi^* \end{pmatrix} \qquad (1.15)$$

Hence, one need only one two-component field φ to define a Majorana particle. In this representation , a Dirac field is a combination of two independent two-components fields :

$$\nu_D = \begin{pmatrix} \varphi \\ -i\sigma^2 \chi^* \end{pmatrix} \qquad (1.16)$$

Using Majorana condition together with the properties of the C matrix, one can show that the CP parity of a Majorana particle can assume the values $\pm i$ and that the vector current of the Majorana field is identically equal to zero: $\overline{\Psi}_M \gamma_\mu \Psi_M = 0$. The latest property is well expected since Majorana field do not carry any additive charge.

The neutrino mass matrix usually originates in gauge theories of electro-weak interaction from Yukawa coupling of the lepton doublets (singlets) with Higgs scalar fields, some component of which develop non-zero vacuum expectation

[1] In chiral representation

$$\gamma_0 = \begin{pmatrix} 0 & \sigma_2 \\ \sigma_2 & 0 \end{pmatrix}, \gamma_1 = \begin{pmatrix} i\sigma_3 & 0 \\ 0 & i\sigma_3 \end{pmatrix}, \gamma_2 = \begin{pmatrix} 0 & -\sigma_2 \\ \sigma_2 & 0 \end{pmatrix}, \gamma_3 = \begin{pmatrix} -i\sigma_1 & 0 \\ 0 & -i\sigma_1 \end{pmatrix}$$

values. In order not to spoil the renormalizability of the theory, these couplings have to be gauge invariant. Thus both Dirac and Majorana mass terms have to be generated in such framework. Dirac mass terms arise most naturally in the standard $SU(2)_L \otimes U(1)_Y$ theory containing right handed neutrino fields $\nu_{l_R}(x)$ as $SU(2)_L$ singlets.

The electro-weak Lagrangian can be completed by the following term:

$$L_2' = -\sum_l G_{\nu_l}(\nu_l, l)_L \, \phi \nu_{l_R} + \text{h.c} \tag{1.17}$$

where h.c denotes for the hermitian conjugate, ϕ is the Higgs doublet introduced in the generation of electron mass from which we deduce: $m_{\nu_l} = \frac{G_{\nu_l} v}{\sqrt{2}}$.

However, this way of generating neutrino mass does not explain the great disparity between the lepton masses and their corresponding neutrinos. In the construction of mass terms, components of opposite chiralities are needed . For particles which are identical with their corresponding antiparticles, opposite chiralities fields can also be introduced by considering the charge conjugate of the original field. Majorana neutrino mass term, which is indeed based on ν and ν^C, cannot be generated naturally in the framework of the MSM. Indeed the product $(C^{-1}\nu_{l_L})^T \nu_{l_L}$ changes the weak isospin by one unit and the only Higgs field which is available is an isodoublet. However, if a triplet of neutral, charged, and doubly charged Higgs field which is conveniently expressed in a matrix form as:

$$H = \begin{pmatrix} -H^+/\sqrt{2} & H^{++} \\ H^0 & H^+/\sqrt{2} \end{pmatrix} \tag{1.18}$$

whose neutral component has a nonzero vacuum expectation value , $\langle H^0 \rangle_0 = v/\sqrt{2}$, is introduced , the gauge invariant coupling :

$$L = \frac{1}{\sqrt{2}} \sum_{l,l' = e,\mu,\tau} h_{l,l'} \left(\bar{\nu}_{l'_L}, \bar{l}'_L \right) H^+ i\tau_2 \begin{pmatrix} \left(\nu_{l_L}\right)^C \\ \left(l_L\right)^C \end{pmatrix} + h.c \qquad (1.19)$$

where $h_{l,l'}$ are symmetric complex numbers leads to the following mass term:

$m_{l,l'} = v\, h^*_{l,l'}$

The general Lagrangian mass term can be written as follows:

$$\begin{aligned} L_M = & -M_D \left[\bar{\Psi}_L \Psi_R + h.c \right] \\ & - \frac{M_L}{2} \left[\overline{(\Psi^c)_R} \Psi_L + h.c \right] \\ & - \frac{M_R}{2} \left[\overline{(\Psi^c)_L} \Psi_R + h.c \right] \end{aligned} \qquad (1.20)$$

To illustrate the physical meaning of such formulation, consider the following fields:

$$f = \frac{\Psi_L + (\Psi_L)^C}{\sqrt{2}} \quad ; \; F = \frac{\Psi_R + (\Psi_R)^C}{\sqrt{2}} \qquad (1.21.a)$$

Notice that : $f^C = f$ and $F^C = F$

Using the properties of the C matrix, one can show that:

$$\begin{aligned} & \left(\Psi_{L,R}\right)^C = (\Psi^C)_{R,L} \\ \text{and } & \overline{(\Psi^C_L)}(\Psi^C)_R = \overline{(\Psi_R)^C}(\Psi_L)^C = \bar{\Psi}_L \Psi_R \end{aligned} \qquad (1.21.b)$$

It can be seen that the charge conjugation operator changes the chirality of the field. The first term in L_M, usually known as the Dirac term, conserves the lepton charge

whereas the others do not.Completing L_M with the kinetic terms associated with the kinetic terms associated with f and F,

$$L = \bar{f}\gamma^{\mu}\partial_{\mu} f + \bar{F}\gamma^{\mu}\partial_{\mu} F - \left(\bar{f},\bar{F}\right)\begin{bmatrix} M_L & M_D \\ M_D & M_R \end{bmatrix}\begin{pmatrix} f \\ F \end{pmatrix} \tag{1.22}$$

The diagonalization of the mass matrix gives the mass eigenvalues associated with the eigenstates ν and N. They are as it follows:

$$m_{\substack{\nu \\ N}} = \frac{1}{2}\left[\left(M_L + M_R\right) \mp \sqrt{\left(M_L - M_R\right)^2 + 4M_D^2}\right] \tag{1.23}$$

$$\begin{pmatrix} \nu \\ N \end{pmatrix} = \begin{pmatrix} \cos\theta & -\sin\theta \\ \sin\theta & \cos\theta \end{pmatrix}\begin{pmatrix} f \\ F \end{pmatrix}$$

$$\text{where} \quad \operatorname{tg} 2\theta = \frac{2M_D}{\left(M_L - M_R\right)}$$

The interesting case is when $M_R >> M_D$. In this case the masses of ν and N are given by:

$$m_{\nu} \approx \frac{M_D^2}{M_R} \quad , m_N \approx M_R \tag{1.24}$$

the two masses differ enormously. Furthermore the mixing angle θ approaches zero so that ν and N are completely decoupled.ν could represent the neutrino. This is known as the seesaw mechanism. It is by far the best explanation of smallness of the neutrino mass.

I-3: NEUTRINO MAGNETIC MOMENT:

I-3-1: Limits on the neutrino magnetic moment:

If the neutrino has a nonzero magnetic moment, then it will undergo a spin flip, when passing through the convective zone. Left handed neutrinos would rotate into right handed ones[7,8]. This effect is more appreciable when the following condition is fulfilled:

$$\mu_\nu \, Bx \approx 1 \qquad (1.25)$$

μ_ν noting the neutrino magnetic moment, B the solar magnetic field amplitude and x the neutrino travelled distance.

The solar convective zone is 2.10^6 km wide, the local magnetic field is expected to be of the order of 10^4 G. For condition (1.25) to be satisfied, μ_ν must be of the order of $10^{-11}\,\mu_B$. However, the allowed magnetic moment for Dirac neutrino in the minimally extended SM is far from the above value, it is just of $10^{-19}\,\mu_B$. Two kinds of magnetic moment can be associated with the neutrino, direct magnetic moment and/or a transitional one. Before proceeding with the discussion of the electromagnetic properties of the neutrino, let us check the present experimental limits[2,12].Constraints come usually from laboratory experiment, astrophysics and cosmology:

Table 2

	upper limit in $10^{-10}\,\mu_B$
Laboratory experiments	$\mu(\nu_e) \rightarrow 10.8$ $\mu(\nu_\mu) \rightarrow 7.4$ $\mu(\nu_\tau) \rightarrow 5.4\ 10^3$
SN 1987A	10^{-2} - 10^{-3}
Nucleosynthesis	0.1

From (ν_e e) scattering experiments, an additional diagram enters in the calculation of the cross section due to the non vanishing magnetic moment . The additional term in the total cross section is magnetic moment dependent, $\sigma_{tot} = \sigma_{W,Z} + \sigma_{\gamma}$.

The astrophysical constraints arise from the estimation of the energy loss due to neutrino pair emission. From stellar collapse, they are different ways to obtain constraints on μ_ν: the fact that all of the observed neutrinos events are clustered with in a time of 10-12 seconds can be explained by the a non massless neutrino. From an other side, neutrinos are supposed to carry out all of the gravitational binding energy released in the process of core collapse. In the presence of the magnetic moment interaction, the ν_{e_L} in the supernova core will scatter against electrons and protons to produce right handed electron neutrino (this is why transition magnetic moment is free from supernovae constraints). Once the ν_{e_R} is produced, it can interact with matter mainly via it magnetic moment. Hence the energy brought by ν_{e_R} can be deduced. The latest is estimated to be of about the third of the total binding energy released in the process of the core collapse, a limit on the magnetic moment can then be set.

I-3-2: Electromagnetic properties of neutrinos:

Physical differences between Dirac and Majorana neutrinos are well exhibited in their electromagnetic properties[2,13].

For charged fermions, basic interaction Lagrangian contains a term: $L_{int} = Q\,\overline{\Psi}\gamma_\mu \Psi A^\mu$, where Q is the charge of the relevant particle. For uncharged fermion, the interaction arise only from loops and is therefore momentum dependent. The effective Lagrangian can be written in analogy with the above term as: $L_{eff} = \overline{\Psi}\,\Sigma_\mu \Psi A^\mu$. Subject to hermiticity condition, the conservation of the electromagnetic current and the consistency with Lorentz covariance, the general form of Σ_λ is:

$$\Sigma_\lambda(p,p') = \left(q^2\gamma_\mu - q_\lambda \not{q}\right)\left[R(q^2)+r(q^2)\gamma_5\right] + \sigma_{\lambda\rho}\,q^\rho\left[D_M(q^2)+iD_E(q^2)\gamma_5\right] \tag{1.26}$$

where R, r, D_M, D_E define the form factors.

Because of translational invariance, Σ_λ depends only on the photon momentum. The physical significance of the form factors can be understood by considering the nonrelativistic limit ($\vec{q}^2 \to 0$). Thus $D_M(0)$ can be identified with the magnetic moment of the particle, $D_E(0)$ with the electric dipole moment, $R(0)$ is called the charged radius and r (0) is the axial charge radius. The latest vanishes in the nonrelativistic limit because of the electric charge neutrality. In the case of Dirac particles all of the four factors are nonzero. No particular condition is assigned to the particle field. However, in the case of Majorana particle, and because of the identification of the particle with the antiparticle, the only nonzero form factor is $r(q^2)$.

In the $SU(2)_L \otimes U(1)_Y$ model, the one loop diagrams mediated by W-boson which give rise to neutrinos magnetic moment are as follows:

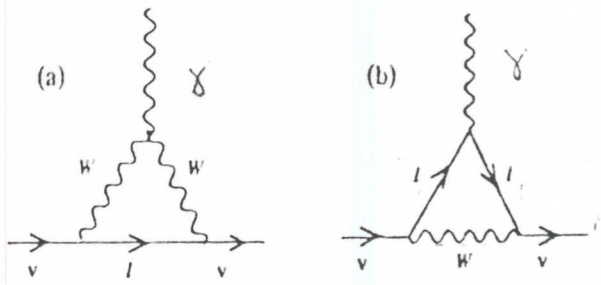

However, neutrino magnetic moment arising from such diagrams will necessarily be proportional to the mass of the external fermion. Indeed, the right chiral projections of the fermions are $SU(2)_L$ singlets, they do not have any

interaction with $W^{\pm}$.Hence, it seems that only the left chiralities are flowing on the neutrino line. To obtain a chirality changing contribution, we must then put a mass insertion on the external legs. Requiring a large magnetic moment seems to be forbidden by the smallness of neutrino mass. Extended models have been considered. Let us turn out to the case of Majorana neutrino. In such case, for each of the above diagrams, their exists a second one in which all of the internal lines are replaced by their conjugate lines. Such contribution is absent in the case of Dirac neutrino. To determine the contribution from the conjugate diagrams, we notice that the charged current interaction in the leptonic sector can be written as follows:

$$\begin{aligned} L_{cc} &= \frac{g}{\sqrt{2}} \sum_{l} \left(\bar{\nu}_L \gamma^{\mu} P_L \ell W_{\mu}^{+} + \bar{\ell} \gamma^{\mu} P_L \nu_l W_{\mu}^{-} \right) \\ &= \frac{g}{\sqrt{2}} \sum_{l} \sum_{\alpha} \left(U_{l\alpha}^{*} \bar{\nu}_{\alpha} \gamma^{\mu} P_L \ell W_{\mu}^{+} + U_{l\alpha} \bar{\ell} \gamma^{\mu} P_L \nu_{\alpha} W_{\mu}^{-} \right) \end{aligned} \tag{1.27}$$

where $P_L = \frac{1-\gamma_5}{2}$ is the left chirality projection operator,U is the mixing matrix defined in (2.2.a).

Using the definition of the conjugate field, L_{cc} can be rewritten in the form:

$$L_{cc} = \frac{g}{\sqrt{2}} \sum_{l,\alpha} \left(U_{l,\alpha}^{*} \bar{\nu}_{\alpha} \gamma^{\mu} P_L \ell W_{\mu}^{+} - U_{l,\alpha} \overline{(\nu_{\alpha})^{C}} \gamma^{\mu} P_R (\ell)^{C} W_{\mu}^{-} \right) \tag{1.28}$$

For Majorana neutrinos, one can use the proportionality between ν_α and $(\nu_\alpha)^C$, to write:

$$L_{cc} = \frac{g}{\sqrt{2}} \sum_{l,\alpha} \bar{\nu}_{\alpha} \gamma^{\mu} \left(U_{l,\alpha}^{*} P_L \ell W_{\mu}^{+} - \lambda_{\alpha} U_{l,\alpha} P_R (\ell)^{C} W_{\mu}^{-} \right) \tag{1.29}$$

Calculating the decay rate one can show that the direct neutrino magnetic moment vanishes.

CHAPTER 2

NEUTRINO CONVERSION:

In this chapter, we will be interested only in the known neutrino generations.

2-1: RESONANT CONVERSION NEUTRINO IN MATTER:

The principal idea governing the possibility of the matter conversion effect is already known for the quark sector. Mass eigenstates can be distinguished from the flavor eigenstates [17,18].

2-1-1: Vacuum oscillation:

We denote by $\upsilon^{(P)}$ the Hamiltonian eigenstate,

$$\nu^{(p)} \equiv \begin{pmatrix} \nu_1 \\ \nu_2 \end{pmatrix} \tag{2.1}$$

We are going to consider the case of two generations. The flavor states are related to the mass eigenstates through a mixing matrix U:

$$\nu^{(f)} \equiv \begin{pmatrix} \nu_e \\ \nu_\mu \end{pmatrix} = U \begin{pmatrix} \nu_1 \\ \nu_2 \end{pmatrix} \tag{2.2.a}$$

where $$U = \begin{pmatrix} \cos\theta & \sin\theta \\ -\sin\theta & \cos\theta \end{pmatrix} \tag{2.2.b}$$

U being the mixing matrix.

The equation of evolution of the state $\upsilon^{(P)}$ is:

$$i\frac{d}{dt}\nu^{(P)}(t) = H\nu^{(P)}(t) \tag{2.3}$$

From the definition of $\upsilon^{(P)}$ it can be seen that H is diagonal in this basis. Even if neutrinos are not massless, their masses will be less important than their energies. The following approximation is thus justified:

$$E_\alpha \equiv E_{1,2} = \sqrt{p^2 + m_\alpha^2} \approx |p| + \frac{1}{2}\frac{m_\alpha^2}{|p|} \tag{2.4}$$

$$H = \begin{pmatrix} |p| + \dfrac{m_1^2}{2|p|} & 0 \\ 0 & |p| + \dfrac{m_2^2}{2|p|} \end{pmatrix}$$

The equation of evolution for $\upsilon^{(f)}$ can be deduced from that of $\upsilon^{(p)}$:

$$i\frac{d}{dx}\nu^{(f)} = H'\nu^{(f)}$$

where $H' = UHU^+$

$$= |p| + \frac{m_1^2 + m_2^2}{4|p|} + \frac{\Delta}{4|p|}\begin{pmatrix} -\cos 2\theta & \sin 2\theta \\ \sin 2\theta & \cos 2\theta \end{pmatrix} \tag{2.5}$$

$$\Delta = m_2^2 - m_1^2$$

The diagonal term in H' enters in the phase factor of the solution, thus it can be omitted. Hence:

$$H' = \frac{\Delta}{4E}\left(\sigma_1 \sin 2\theta - \sigma_3 \cos 2\theta\right) \tag{2.6}$$

where we write $|p|$ simply as E, σ_i denote for the Pauli matrices.

The mixing angle is the angle that diagonalize H', it is given by:

$$\mathrm{tg}(2\theta) = \frac{2H'_{12}}{H'_{22} - H'_{11}}$$

$$\text{hence } \nu^{(f)}(x) = \exp(-iH'x)\,\nu^{(f)}(0) \qquad (2.7)$$

$$= (\cos\frac{\Delta x}{4E} - i(\sigma_1 \sin 2\theta - \sigma_3 \cos 2\theta)\sin\frac{\Delta x}{4E})\,\nu^{(f)}(0)$$

the probability of the evolution of an electron neutrino to a muonic neutrino is given by:

$$P_{\nu_e \to \nu_\mu}(x) = \sin^2 2\theta \, \sin^2 \frac{\Delta x}{4E} \qquad (2.8)$$

It is clear from this expression that the transition probability will be meaningless when neutrinos are massless.

2-1-2: Neutrino oscillation in uniform matter:

How about neutrino oscillation in matter?

The main difference is in the dispersion relation. It is modified by the interaction terms. In solar matter, neutrinos interact with electrons, protons and neutrons via neutral (a) or charged (b) currents.

Charged current interaction: CC

With regard to the central temperature of the sun ($\sim 10^7$ K), the impulsion of the boson W can be neglected relatively to its mass. The interaction term takes the following form:

$$L_{eff} = -\frac{4G_F}{\sqrt{2}}\left\{\bar{e}_L(p_1)\gamma^\mu \nu_{e_L}(p_2)\right\}\left\{\bar{\nu}_{e_L}(p_3)\gamma_\mu e_L(p_4)\right\} \qquad (2.9.a)$$

Using the Fierz transformation and assuming that neutrino impulsion does not change considerably:

$$L_{eff} = -\frac{4G_F}{\sqrt{2}}\left\{\bar{e}_L(p_1)\gamma^\mu e_L(p_4)\right\}\left\{\bar{\nu}_{e_L}(p)\gamma_\mu \nu_{e_L}(p)\right\} \qquad (2.9.b)$$

Written in this form, Leff represents a neutrino current propagating in an electron medium. Averaging over three electron current:

$$L_{eff} = \left\langle \bar{e}_L \gamma_\mu e_L \right\rangle \bar{\nu}_{e_L}\gamma^\mu \nu_{e_L}$$
$$\left\langle \bar{e}_L \gamma_\mu e_L \right\rangle = 1/2 \left\langle \bar{e}\gamma_\mu e \right\rangle - 1/2 \left\langle \bar{e}\gamma_\mu\gamma_5 e \right\rangle \qquad (2.10.a)$$

the spatial component of the Dirac current is assumed to be zero, electron velocity distribution being a Maxwellien. We assume also that the electrons are not particularly polarized, $\left\langle \bar{e}\gamma_\mu\gamma_5 e \right\rangle = 0$. Hence L_{eff} reduces to:

$$L_{eff} = -\sqrt{2}\, G_F\, n_e \left(\bar{\nu}_{e_L}\gamma_0 \nu_e\right) \qquad (2.10.b)$$

where n_e is the electron density. Muons do not enter in the above term. Since solar conditions do not allow their generation.

Neutral current interaction: NC

The Lagrangian of the interactions proceeding via neutral current is given by:

$$L_{eff} = -\frac{4G_F}{\sqrt{2}}\left\{\bar{f}(p_1)\gamma^{\mu}\left(\tau_3\left(\frac{1-\gamma^5}{2}\right) - Q\sin^2\theta_W\right) \quad f(p_2)\right\}\bar{\nu}_L(p)\,\gamma_{\mu}\,\nu_L(p) \tag{2.11.a}$$

where f denotes a nucleon or an electron.

Averaging L_{eff} as before over the velocity and the polarization of the solar matter, the contributions of the protons and electrons cancel in a neutral medium, because of their opposite electric charges and weak isospin.

$$L_{eff} = \frac{G_F}{\sqrt{2}} n_n \sum \bar{\nu}_L^{\ell}\gamma_0\nu_L^{\ell} \tag{2.11.b}$$

where ℓ represent any neutrino type.

The superposition of the two types of interaction gives:

$$L_{eff} = -\sum \bar{\nu}_L^{l}\,\gamma_0\,V_{\nu_l}\,\nu_L^{l} \tag{2.12}$$

where

$$V_{\nu_e} = \sqrt{2}\,G_F\left(n_e - \frac{1}{2}n_n\right)$$

$$V_{\nu_\mu} = -\frac{1}{\sqrt{2}}G_F\,n_n$$

n_n is the neutron density.

$$\begin{aligned}\tilde{H}' &= H' + \begin{pmatrix} V_{\nu_e} & 0 \\ 0 & V_{\nu_\mu}\end{pmatrix} \\ &= E + \frac{m_1^2 + m_2^2}{4E} - \frac{1}{\sqrt{2}}G_F n_n + \frac{1}{4E}\begin{pmatrix} -\Delta\cos 2\theta + 4\sqrt{2}\,G_F\,n_e E & \Delta\sin 2\theta \\ \Delta\sin 2\theta & \Delta\cos 2\theta\end{pmatrix}\end{aligned} \tag{2.13}$$

The angle that diagonalizes $\tilde{H}'$ define the angle of oscillation in matter, it is given by:

$$\mathrm{tg}2\tilde{\theta} = \frac{2\tilde{H}_{12}}{\tilde{H}_{22} - \tilde{H}_{11}} = \frac{\Delta \sin 2\theta}{\Delta \cos 2\theta - A} \quad ; \qquad (2.14.a)$$

$$A = 2\sqrt{2} G_F E n_e$$

The mixing angle $\tilde{\theta}$ is maximal for $A = \Delta \cos 2\theta$, otherwise for an electron density such that $n_e = \frac{\Delta \cos 2\theta}{2\sqrt{2} G_F E}$, the mixing is maximal. From an other hand, the transition probability is proportional to $\sin^2 2\theta$, the relation giving $\mathrm{tg}2\tilde{\theta}$ can be rewritten in the form:

$$\sin^2 2\tilde{\theta} = \frac{\Delta^2 \sin 2\theta}{(\Delta \cos 2\theta - A)^2 + \Delta^2 \sin^2 2\theta} \qquad (2.14.b)$$

Thus, the probability reaches a resonance at $A = \Delta \cos 2\theta$, the width of the resonance is given by: $\Gamma = \Delta \sin 2\theta$. Mikheyev and Smirnov first realized the importance of the presence of such a resonance in the context of the solar neutrino puzzle.

2-1-3: Neutrino oscillation in non uniform matter:

The study of this case is important for the case of solar matter distribution. The evolution of the state $\nu^{(f)}$ is given by the equation:

$$i \frac{d}{dx} \nu^{(f)} = \frac{1}{2E} \tilde{M}^2 \nu^{f)} \qquad (2.15.a)$$

where $\tilde{M}^2$ is the term not proportional to the matrix unity.

$$i\frac{d}{dx}\tilde{\nu}^{(p)} = \left(\frac{1}{2E}\tilde{U}^{+}\tilde{M}^{2}\tilde{U} - i\tilde{U}^{+}\frac{d\tilde{U}}{dx}\right)\tilde{\nu}^{(p)}$$

$$i\frac{d}{dx}\begin{pmatrix}\tilde{\nu}_1\\ \tilde{\nu}_2\end{pmatrix} = \begin{pmatrix}\frac{\tilde{m}_1^2}{2E} & i\frac{d\tilde{\theta}}{dx}\\ -i\frac{d\tilde{\theta}}{dx} & \frac{\tilde{m}_2^2}{2E}\end{pmatrix}\begin{pmatrix}\tilde{\nu}_1\\ \tilde{\nu}_2\end{pmatrix} \qquad (2.15.b)$$

where $\tilde{m}_{1,2}$ are the eigenvalues of $\tilde{H}'$.

In the case of uniform matter $\frac{d\tilde{\theta}}{dx} = 0$, the system (2.15.b) reduces to (2.13). Otherwise the possibility of transition of $\tilde{\nu}_1$ *to* $\tilde{\nu}_2$ has to be considered.

Adiabaticity condition :

First of all we are going to quantify the adiabatic conditions. The evolution of a physical state $\tilde{\nu}_1$ is said to be adiabatic if doesn't suffer from any transmutation.

$$\left|\frac{d\tilde{\theta}}{dx}\right| << \frac{\left|\tilde{m}_1^2 - \tilde{m}_2^2\right|}{2E}$$

or

$$\left|\frac{d\tilde{\theta}}{dx}\right| = \sqrt{2}G_F E\frac{\Delta\sin 2\theta}{(\Delta\cos 2\theta - A)^2 + \Delta^2\sin^2 2\theta}\left|\frac{dn_e}{dx}\right| \qquad (2.16.a)$$

$$<< \frac{\left[(\Delta\cos 2\theta - A)^2 + \Delta^2\sin^2 2\theta\right]^{1/2}}{2E}$$

Defining the adiabaticity parameter γ by:

$$\gamma(x) = \frac{(\Delta/E)^2}{2\sqrt{2}G_F} \frac{\sin^2 2\theta}{\sin^2 2\tilde{\theta}} \frac{1}{\left|\frac{dn_e}{dx}\right|} \tag{2.16.b}$$

the adiabaticity criteria sets that : $\gamma(x) >> 1$ (2.16.c)

From (2.16.b) one can see that the propagation is said to be adiabatic when the matter density changes sufficiently slowly. If the variation is important transition between mass eigenstates became possible.

We suppose that the conditions of adiabaticity are fulfilled so that we can neglect the non diagonal elements. The evolution of the state $\tilde{\nu}_\alpha$ is given by:

$$\begin{aligned} \tilde{\nu}_\alpha(x) &= \exp\left(-i\int_0^x dx' \tilde{E}_\alpha(x')\right)\tilde{\nu}_\alpha(0) \\ P^{(ad)}_{\nu_e \to \nu_e} &= \left|\langle \nu_e(x) | \nu_e(0)\rangle\right|^2 \\ &= \left|\sum_{\alpha,\alpha'} \langle \nu_e(x) | \tilde{\nu}_\alpha(x)\rangle\langle \tilde{\nu}_\alpha(x) | \tilde{\nu}_{\alpha'}(0)\rangle\langle \tilde{\nu}_{\alpha'}(0) | \nu_e(0)\rangle\right|^2 \end{aligned} \tag{2.17}$$

Under such conditions, no transition between $\tilde{\nu}_\alpha$ *and* $\tilde{\nu}_{\alpha'}$ is possible. The summation reduces to α. Averaging over all the possible energies, one gets:

$$P^{(ad)}_{\nu_e \to \nu_e}(x) = 1/2\left(1 + \cos 2\tilde{\theta}_0 \cos 2\theta\right) \tag{2.18}$$

where $\tilde{\theta}_0$ is the mixing angle where neutrino is produced.

Non adiabatic solution:

We denote by X, the probability of oscillation of $\tilde{\nu}_1$ *to* $\tilde{\nu}_2$. The survival probability of an electron neutrino is :

$$P_{\nu_e \to \nu_e} = 1/2\left[1 + (1 - 2X)\cos 2\tilde{\theta}_0 \cos 2\theta\right] \tag{2.19}$$

The problem of the calculation of diverse probabilities is then reduced to the determination of P_R

Calculation of P_R :

The Landau - Zener method [19] for the calculation of the non adiabatic transition probability between two states sets that:

$$\mathrm{Ln}\, P_R = \mathrm{Ln}\, P_{LZ} = -2\,\mathrm{Im}\left[S_1(t_1, t_0) + S_2(t_0, t_2)\right] \tag{2.20}$$

where $S_1(t_1, t_0)$ denotes the action for the motion of the neutrino beam in state $\tilde{\nu}_1$ from some initial time t_1 to a transition time t_0, t_2 being the time when the neutrino goes out of the non-adiabatic region.

$$Ln\, P_{LZ} = -2\,\mathrm{Im}\left[\int_{t_R}^{t_0} dt\,\left(\tilde{E}_2 - \tilde{E}_1\right)\right] \tag{2.21.a}$$

$$t_R = t_1 = t_2$$

expressed in terms of A,

$$Ln\, P_{LZ} = -\frac{1}{E}\,\mathrm{Im}\left(\int_{A_R}^{A_0} \frac{dA}{(dA/dx)}\left[\left(\Delta\cos 2\theta - A\right)^2 + \Delta^2 \sin^2 2\theta\right]^{1/2}\right) \tag{2.21.b}$$

Using this method, A_0 is the value of A for which $\tilde{E}_1 = \tilde{E}_2$. For a linear variation of A in terms of x, P_{LZ} is given by:

$$\mathrm{Ln}\,P_{LZ} = -\frac{\pi\,\Delta\sin^2 2\theta}{4E\cos 2\theta}\,\frac{1}{\left|\frac{d}{dx}\mathrm{Ln}\,A\right|_R} \tag{2.22}$$

Hence,

$$P_{LZ} = \exp\left(-\frac{\pi}{4}\gamma_R\right)$$

2.2: RESONANT SPIN FLIP PRECESSION:

The resonant matter precession effect is based on the fundamental assumption of non zero neutrino mass. An other effect based on a non vanishing magnetic moment is considered.

2.2.1: Spin effect:

To illustrate this effect, consider the simple case of the evolution of the states (ν_L, ν_R):

$$i\frac{d}{dx}\begin{pmatrix}\nu_L\\ \nu_R\end{pmatrix} = \begin{pmatrix}0 & \mu B\\ \mu B & 0\end{pmatrix}\begin{pmatrix}\nu_L\\ \nu_R\end{pmatrix} \tag{2.23}$$

hence, the survival probabilities for a constant and a time dependent magnetic fields are given respectively by:

$$P_{\nu_L\to\nu_L}(x) = \cos^2(\mu B x) \tag{2.24}$$

Note that the above expressions of the survival probabilities do not depend on energy, whereas the matter resonant expression does (2.14.a, 2.14.b). If this effect was the dominant effect that affects neutrinos propagation, the neutrino suppression must be the same for the different neutrino sources. Spin flip effect has been introduced to explain the observed time variation in the flux detected by Homestake experiment. Since any time variation of the solar magnetic field is supposed to be related to the magnetic field in the convective zone, let us roughly estimate the survival probability for a left handed neutrino propagating through the convective zone. At the minimum of activity, the argument μBx is lower than its value at the maximum activity. The corresponding flux is higher in the first cases than in the second one. Thus an anticorrelation is invoked.

Consider a neutrino with a $10^{-11}\mu_B$ magnetic moment propagating through the convective zone. $P_{\nu_L \to \nu_L}$ passes from unity in the minimum activity to 0.69 at the maximum activity characterized by a magnetic field of the order of 10 kG . Hence, for the suppression rate to be of the order of the observed one (1/3, 1/2) neutrinos should go through a resonant zone.

2.2.2: Resonant spin matter effect:

Consider the evolution of the states $\nu^{(f)} \equiv \left(\nu_e, \bar{\nu}_\mu\right)$ through the sun:

$$i\frac{d}{dx}\begin{pmatrix}\nu_e\\ \bar{\nu}_\mu\end{pmatrix} = H\begin{pmatrix}\nu_e\\ \bar{\nu}_\mu\end{pmatrix} \qquad (2.25.a)$$

To illustrate this effect we are going to consider a zero neutrino vacuum mixing angle. Proceeding as in the case of resonant matter precession we get [20]:

$$H = \begin{pmatrix} a_e(x) & \mu B \\ \mu B & \frac{\Delta^2}{2E} - a_\mu(x) \end{pmatrix} \qquad (2.25.b)$$

where

$$a_e(t) = \frac{G_F}{\sqrt{2}}(2\,n_e - n_n)$$
$$a_\mu(t) = -\frac{1}{\sqrt{2}} G_F\, n_n \qquad (2.25.c)$$
$$n_n \approx \frac{n_e}{6}$$

n_e and n_n are respectively the electron and neutron densities

Diagonalizing H, we define the spin matter mixing angle:

$$\nu^{(p)} = \begin{pmatrix} \cos\theta_{SM} & -\sin\theta_{SM} \\ \sin\theta_{SM} & \cos\theta_{SM} \end{pmatrix} \nu^{(f)}$$

$\nu^{(p)}$ are the eigenvectors of H (2.26)

$$tg2\theta_{SM} = \frac{2\mu B}{\frac{\Delta^2}{2E} - \frac{5\sqrt{2}}{6} G_F\, n_e}$$

where θ_{SM} denotes for the mixing angle.

The mixing angle depends once again on the electron density. It passes through a minimal value corresponding to $\nu_1 \equiv \nu_e$ to a maximal value corresponding to $\nu_1 \equiv \bar{\nu}_\mu$.

Transition probability:

Adiabatic solution:

θ^0_{SM} denotes for the local mixing angle where an electron neutrino is produced. Thus,

$$\nu_e = \nu_1 \cos\theta^0_{SM} + \nu_2 \sin\theta^0_{SM} \qquad (2.27)$$

ν_e is produced in the state ν_1 with the probability $(\cos\theta^0_{SM})^2$. In adiabatic conditions, no oscillation between mass eigenstates is possible. Then, it will be detected as an electron neutrino with the probability $(\cos\theta_{SM})^2$. However, it can be seen from the plot of $\cos 2\theta_{SM}$ in terms of the solar radius, that such condition is fully violated near the resonance, defined by the condition of maximal mixing. The survival probability of an electron neutrino is then given by:

$$P^{(ad)}_{\nu_e \to \nu_e}(x) = \cos^2\theta_{SM}\ \cos^2\theta^0_{SM} + \sin^2\theta^0_{SM}\sin^2\theta_{SM}$$
$$= 1/2\left(1 + \cos 2\theta^0_{SM}\cos 2\theta_{SM}\right) \qquad (2.28)$$

where θ_{SM} is the mixing angle at the edge of the sun

Non-adiabatic solution:

Adiabaticity parameter:

The adiabaticity parameter is defined from the condition of neglecting the off diagonal terms relatively to the diagonal ones, following (2.16.a):

$$\left|\frac{d\theta_{SM}}{dx}\right|_{res} << \left|M^2_{SM_1} - M^2_{SM_2}\right|_{res} \qquad (2.29)$$

From the expression of $tg2\theta_{SM}$ and the fact that in the total extent of the solar matter, the variation of the density is more important than that of the magnetic field - the density varies from 10^2 to 10^{-12} g/cm^3 and the magnetic field from 10^7 at the center to few gauss at the surface - one obtains for γ:

$$\gamma = \frac{(2\mu B)^2}{\frac{\Delta^2}{2E}\left|\frac{d\text{Ln } n_e}{dx}\right|_{res}} \qquad (2.30)$$

Evaluation of transition probability:

According to the method of Landau-Zener, the transition probability is given by:

$$\text{Ln } P_{LZ} = -\frac{2}{\hbar}\text{Im}\int_{t_R}^{t_0} dt\,(M_{SM_2} - M_{SM_1}) \qquad (2.31)$$

where t_R is the time when the neutrino goes through the resonant zone, t_0 the time when it goes out of the non-adiabatic region.

By considering the expressions of $M_{SM_{1,2}}$, and using a linear variation of the electron density we get:

$$\text{Ln } P_{LZ} = -\frac{R_S}{\hbar c}\text{Im}\int_{n_R}^{n_0}\frac{dn}{\left(\frac{dn}{dx}\right)}\sqrt{\left(\frac{\Delta^2}{2E} - n\right)^2 + (2\mu B)^2} \qquad (2.33)$$

where R_S is the solar radius, n_0 is the value of n for which the mass eigenvalues are equal, n_R the value of n at the resonance.

$$\text{Hence: Ln } P_{LZ} = -\frac{R_S E\pi(2\pi B)^2}{\hbar c\Delta^2\left|\frac{d\text{Ln } n}{dx}\right|_{res}} \qquad (2.34)$$

For an exponentially variation of the electron density, the transition probability is given by Petcov formula. Resonance region is independent of the local magnetic field, it's location is given by the same condition as the matter effect, namely

$\frac{5\sqrt{2}}{6}G_F n_e = \frac{\Delta^2}{2E}$ (2.35) , whereas the width of the resonance region is. The width is given by: $\Gamma_{SM} = 2\mu B$, since the probability is proportional to $\sin^2 2\theta_{SM}$ the latest expression can be obtained by rewritten the expression of $tg2\theta_{SM}$. The survival probability of , say an electron neutrino is given by (2.20).

CHAPTER 3

SOLAR STRUCTURE:

The Sun is the well studied star because of it proximity to the Earth. However after decades of work , it is still not certain whether the physics of solar energy generation is as expected. Solar neutrino experiments will bring the final decision. In fact whereas the observed photons are last scattered (or are produced) in the outer 0.05% of the solar radius[4], neutrinos emerge directly from the solar core.

3.1- Thermonuclear reactions:

The life history of a star is an interplay between the gravitational, the electromagnetic and the strong nuclear forces. Main sequence stars burn their hydrogen, the large Coulomb repulsion slows the nuclear reaction rates to an astronomically long time scales. The determination of some nuclear reaction rates is still uncertain (see table 2). The relevant energies are so low that the laboratory event rates are small. This is a source of uncertainty in the calculation of stellar models. The reaction rate enters, obviously, in the calculation of energy released by the thermonuclear reactions. It gives the number of reactions per unit volume per unit of time. It is described by the formula [21]:

$$R_{12} = \frac{n(1)\ n(2)}{1+\delta_{12}} \langle \sigma\ v \rangle_{12} \qquad (3.1)$$

where n(1), n(2) are the number densities of particles of type 1 and 2, σ is their interaction cross section, v the magnitude of their relative velocity and the Kronecker symbol is there to prevent double counting the identical particles.

$$\sigma(E) = \frac{S(E)}{E} \exp(-2\pi\eta) \tag{3.2}$$

where

$$\eta = Z_1 Z_2 e^2 / \hbar v$$

The value of S (E) at zero energy is known as the cross section factor S_0. It is of great importance in the determination of cross sections at thermal energies . Usually, cross sections are measured at energies of the order of the Mev. Using equation (3.2) the cross sections at thermal energies can be parametrized. These computations are important for the computation of the rate at which nuclear reactions contribute to the total energy output of a star. It is given by:

$$\varepsilon = \sum_r (Q - \bar{q})_r R_r \tag{3.3}$$

where Q is the total thermal energy released, $\bar{q}$ the average neutrino energy loss and R_r for the reaction rate.

Thermonuclear reactions can be set into two chains: the pp chain and the CNO chain.

The proton-proton chain is summarized in the following table [4]:

Table 3

Reaction	ν Flux ($cm^{-2} s^{-1}$)	Energy (Mev)	Characteristics
$p + p \rightarrow {}^{2}H + e^{+} + \upsilon e$	6.10^{10}	≤ 0.42	The basis of the whole PP chain after which follows the name ofthe chain.
$p + e^{-} + p \rightarrow {}^{2}H + \upsilon e$	$1.5\ 10^{8}$	1.442	
${}^{2}H + p \rightarrow {}^{3}He + \gamma$			so fast that it rate is not important
${}^{3}He + {}^{4}He \rightarrow {}^{7}Be + \gamma$ or ${}^{3}He + {}^{3}He \rightarrow \alpha + 2p$			leads to the production of ${}^{7}Be$ which is an important source of neutrinos
${}^{7}Be + e^{-} \rightarrow {}^{7}Li + \upsilon e$	4.10^{9}	90% (0.86 10% (0.38	
${}^{7}Li + p \rightarrow 2\alpha$ or ${}^{7}Be + p \rightarrow {}^{8}B + \gamma$			occurs rarely (0.02%) but it is of crucial importance since it leads to the most energetic ˘B neutrinos. Its cross section is however not well estimated.
${}^{8}B \rightarrow {}^{8}Be^{*} + e^{+} + \upsilon e$ ${}^{8}Be^{*} \rightarrow 2\alpha$ or ${}^{3}He + p \rightarrow {}^{4}He + e^{+} + \upsilon e$	$5.8\ 10^{6}$ $7.6\ 10^{3}$	< 15 ≤ 18.77	

The astrophysical factors for the reactions $^{3}He(\alpha,\gamma)^{7}Be$ and $^{7}Be(p,\gamma)^{8}B$, S_{34} and S_{17} are the main parameters determining different solar models.

The CNO cycle contributes according to the SSM only by an order of 1.5% to the total solar luminosity, it can be summarized as the conversion of four protons to form an α-particle, two positrons and two neutrinos which is achieved with the aid of ^{12}C, the most abundant heavy isotope.

Table 4

Reaction	υ energy (Mev)
$^{12}C + p \rightarrow {}^{13}N + \gamma$ $^{13}N \rightarrow {}^{13}C + e^{+} + \upsilon e$	≤ 1.199
$^{12}C + p \rightarrow {}^{14}N + \gamma$ $^{14}N + p \rightarrow {}^{15}O + \gamma$ $^{15}O \rightarrow {}^{15}N + e^{+} + \upsilon e$	≤ 1.732
$^{15}N + p \rightarrow {}^{12}C$	

3.2: STELLAR EVOLUTION:

3.2.1: EQUATIONS OF STELLAR EVOLUTION:

The thermodynamical properties of any star can be described by the conservation laws of mass, energy and the equations governing energy transport. For a star in the quasistatic main sequence (or hydrogen burning) like the sun, some simplifying assumptions can be considered. Spherical symmetry and quasistatic equilibrium without material convection are quantitatively accurate for constructing models of stellar interiors. Rotation and magnetic fields are not considered [4,21,22] since rotational and magnetic energies are negligible compared to thermal energy.

The equation of hydrostatic equilibrium describes the balance between the gravitational and pressure force:

$$\frac{dP(r)}{dr} = -\frac{GM(r)\rho(r)}{r^2} \tag{3.4}$$

where $P(r)$ and $\rho(r)$ are the total pressure (radiative and thermal) and density at a distance r from the center of the star and M(r) the enclosed mass.

$$P(r) = \frac{a}{3}T^4 + \frac{1}{\mu}\frac{k\rho T}{m_H} \tag{3.5}$$

where μ is the mean molecular weight, $\mu^{-1} = 2X + \frac{3}{4}Y + \frac{1}{2}Z$

X, Y, Z being the fractions by mass of hydrogen, helium and heavier elements, a is the Stefan Boltzman constant.

Nuclear energy supplies both the radiated luminosity and the local heat which supports the star against gravitational contraction.

$$\frac{dL_r}{dr} = \rho\ (4\pi r^2\ )\left(\varepsilon_{nuclear} - T\frac{dS}{dt}\ \right) \tag{3.6}$$

where S is the stellar entropy.

The diffusion of this energy (luminosity) is guaranteed by the presence of a temperature gradient. The energy transport can be either via a convective mode, a radiative or conductive modes. In the absence of motion radiative transport is favored. The repeated absorption and emissions rise the local temperature . It creates a temperature gradient which intensity is proportional to the radiation flux $L/4\pi r^2$ and inversely proportional to the mean free path of the photons ℓ.

$$\frac{dT}{dr} = -\left(\frac{3}{16\,T^3 a}\right)\left(\frac{L_r}{4\pi r^2 \ell}\right) \tag{3.7}$$

where 'a' is the Stefan-Boltzman cconstant. Written in an other way:

$$L_r = -4\pi r^2 \frac{4a}{3} \frac{1}{\kappa\rho} \frac{dT^3}{dr} \tag{3.8}$$

κ is the total opacity, it is the combination of a radiative and the conductive opacities: $\kappa^{-1} = \kappa_{rad}^{-1} + \kappa_{cond}^{-1}$. The solar interior is dominated by the radiative opacity.

3.2.2: STANDARD SOLAR MODEL:

The study of the physics of the sun is a way to explore the star's core to verify the validity of the known theories of stellar structure. We are going to give a brief description of the fundamental parameters that enters in the development of SSM. The assumptions given above of spherical symmetry , hydrostatic equilibrium and that of neglecting the effects of rotation and magnetic field are considered [23,24]. The elaboration of solar models can be summarized in the resolution of the equations of stellar structure, generally expressed in terms of the M_r enclosed mass in the sphere of radius r. We have to determine the time evolution of the pressure, temperature, radius, luminosity and the mass abundance of the different elements: $P(M_r , t)$, $T(M_r , t)$, $r(M_r , t)$, $L_r(M_r , t)$, $\chi_i(M_r , t)$. The variation of each element is altered by the producing reactions and the destructive ones. Hence it is given by:

$$\frac{\partial X_i}{\partial t} = -\sum_{k'} \frac{\varepsilon_{k'}}{Q_{ik'}} + \sum_{k''} \frac{\varepsilon_{k''}}{Q_{ik''}} \tag{3.11}$$

where $Q_{ik'}$ is the energy released (absorbed) when 1g of the i^{th} element is districted (produced) by k' (k") reaction . In the convective zone, one has to take the matter mixing into account (due to the motion of the particles):

$$\frac{\partial X}{\partial t} = \frac{\int_{conv}\left(-\sum_{k'}\frac{\varepsilon_{k'}}{Q_{ik'}} + \sum\frac{\varepsilon_{k''}}{Q_{ik''}}\right)}{\int_{conv} dM_r} dM_r \qquad (3.12)$$

We are dealing with a system of non linear differential equations. A satisfactory solar model is then a solution of the evolutionary equations that satisfies boundary conditions in both space and time. The present mass, luminosity and radius of the sun must be finally found.

The predicted energy spectrum of the solar neutrinos is given in (fig 3.1) [4].

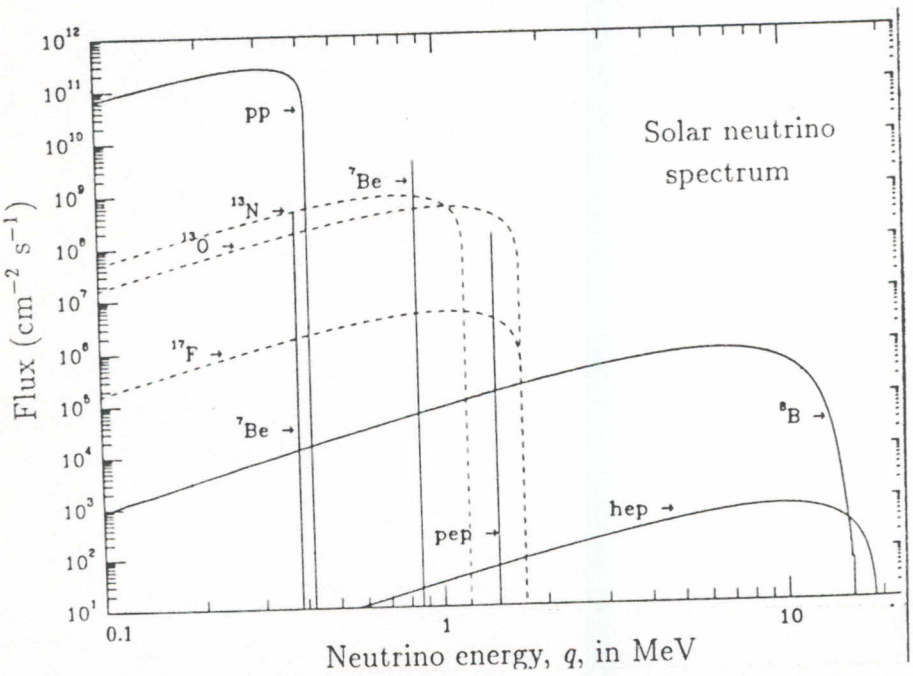

fig(3.1)

The dispersion of the production zone of neutrinos is one of most important results of SSM. It is used in the study of the neutrino deficit to deduce the conditions, neutrinos detected by each of the working experiments are concerned with. It is given in fig(3.2)[4].

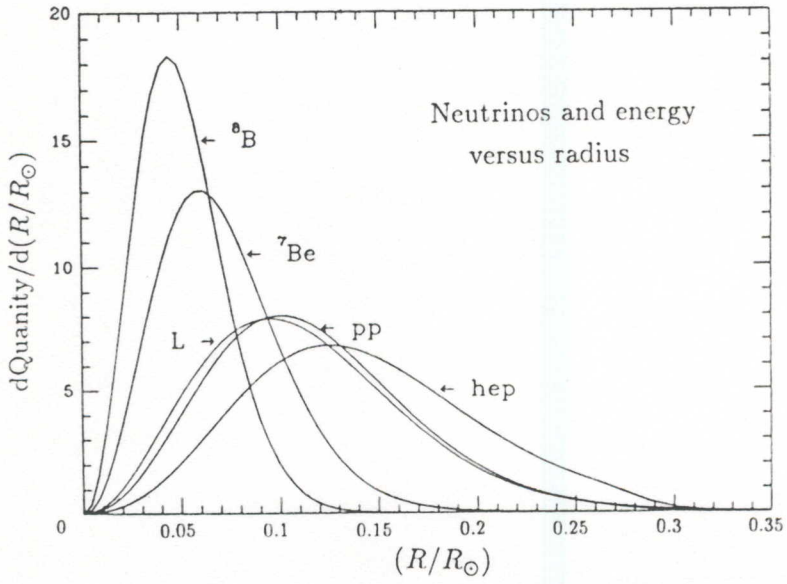

fig(3.2)

The complexity in the elaboration of a stellar code is in the wide range of variation of the density $\left(10^{-12} to 10^{2}\ g/cm^{3}\right)$ and of the temperature $\left(5.10^{3} to 10^{7}\ K\right)$ .The nuclear reactions at the energies equivalent to the solar core energy (10^{7} K $\cong$ 1.3 keV) are not reproducible in laboratory. Their corresponding cross sections are obtained by extrapolation. The factors S_{34} and S_{17} are the most important. They determine the production rate of ^{8}B, the source of the most energetic neutrinos. Convective phenomena, on the other side, are not well understood.

A- Chemical abundances: The chemical abundances of the elements affect the computed radiative opacity and hence the temperature density profile of the solar interior. The sun is assumed to be chemically homogeneous when it reached on the main sequence. The present solar surface composition is assumed to reflect the initial abundances of all of the elements at least as heavy as carbon, the surface temperature being insufficient to favorite any nuclear burning. The initial ratio by mass of elements heavier than helium relative to hydrogen, Z/X, is one of the crucial

input parameters in the determination of a solar model. The fractional abundances of the heavy elements are given in [24].

B- The equation of state: The pressure appearing in the equation of stellar structure is the superposition of the radiative and thermal pressure. A gas has to be considered as perfect when the energy of interaction between the particles is negligible when compared to their thermal energy. This the case for the ions. The pressure due to the electrons is mainly affected by the degrees of ionization of the chemical elements.

C- Radiative opacity: The transport of energy in the central regions of the sun is essentially through photon radiation. The calculated radiative opacity depends upon the chemical composition and upon the modeling of complex atomic processes. Fortunately these calculations are not a major source of uncertainty for solar neutrinos calculations. In fact, the radiative opacity in the central regions of the sun is mainly produced by photon scattering on free electrons and inverse bremsstralung in the presence of completely ionized hydrogen and helium, processes that can be calculated to a good accuracy.

Calculating procedure:

The models of stellar evolution are constructed by integrating the following system:

$$\frac{dP}{dr} = -\rho \frac{G M}{r^2}$$

$$\frac{dM}{dr} = 4\pi r^2 \rho$$

$$\frac{dL}{dr} = 4\pi r^2 \rho \left[\varepsilon - T \frac{dS}{dt} \right] \qquad (3.13)$$

$$\left. \frac{dT}{dr} \right|_R = -\frac{3\kappa\rho}{16 a T^3} \frac{L}{4\pi r^2}$$

$$\left. \frac{dT}{dr} \right|_C = \frac{\Gamma - 1}{\Gamma} \frac{T}{P} \frac{dP}{dr}$$

R denoting for the radiative mode of transfert of energy, C for the convective mode of transfert, Γ for the second adiabatic exponent.

One has to guess an initial set of parameters (X, X/Z), run the model using difference equations to represent the equation of stellar evolution, calculate the predicted characteristics of the present sun; results are iterated until numerical agreement between the model and the observed sun is obtained. The solution of the evolutionary equations determines the values of the mass fractions of hydrogen, helium and heavy elements, the present physical variables inside the sun, the spectrum of acoustic observed oscillation frequencies of the solar surface and, as well, the neutrinos fluxes. The SSM calculations have been refined over years. The model is in good agreement with helioseismology observation. Departure from SSM has been presumed mainly to explain neutrinos flux deficit. Non Standard Solar Models (NSSM) are constructed by modifying the current assumptions or input data.

Table 5

	BP	TL	SS (93)	DS (94)	experim.data
pp (E 10)	6.00	6.02	6.1	6.04	
^{7}Be (E 9)	4.89	4.33	3.9	4.30	
^{8}B (E 6)	5.69	4.43	3.0	2.77	2.90 ± 0.42 Kamiokande
^{13}N (E 8)	4.92	3.83	—	0.747	
^{15}O (E 8)	4.26	3.15	—	0.217	
Homestake (SNU)	8.0 ± 3.0	6.4 ± 1.4	4.5	4.2	2.32 ± 0.23
GALLEX (SNU)	132^{+21}_{-17}	127±7	114	109	79 ± 10 ± 6
SAGE (SNU)	132^{+21}_{-17}	127 ± 7	114	109	69 ± 11 ± 6
Tc (10^{7} K)	1.559	1.549	1.545	1.571	
S_{17} eV . b	24	21	20.2	17	
S_{34} keV . b	0.533	—	—	0.45	

The first column in the table gives the list of physical quantities and of experiments, the second column gives the predictions of the Bahcall and Pinsonneault model, the third column refers to the Turck-Chiese and Lopes model, in the fourth and fifth columns the predictions of the low-flux models (Shi and Schramm and Dar and Shaviv) are listed and the last column gives the experimental data. The neutrino fluxes (pp, Be etc..) are given in units cm^{-2} s^{-1} with the orders of magnitude indicated in the first column.

3.2.3:NON STANDARD SOLAR MODEL:

Before exposing the main ideas that underlay some of the proposed NSSM, let us see why an astrophysical solution of the solar neutrino problem is disfavored

by the present results of the four neutrinos experiments. The most compelling reason for considering the particle physics solution comes from the failure of the present astrophysical solutions to explain the lower Homestake rate when compared to the Kamiokande rate. Astrophysical solutions do not destroy the neutrino energy spectrum. We are allowed to change the amplitude of the ^8B flux, but not to deplete only the lower energy part of the spectrum in order to reconcile the Homestake and Kamiokande rates. However, particle physics solutions are energy dependent. The resonance probability depends on neutrino energy and the experimental results can be well explained in such scenario.

A class of NSSM can be characterized by lower core temperatures. The low Z model modify the opacity[25], the rapid rotation model and the strong magnetic field modify the equation of hydrostatic equilibrium, and the thermal pressure required to support the star against gravity therefore decrease the emitted solar neutrino flux. Neutrino fluxes are described by the power laws of the central temperature T_C [4]:

$$\Phi(pp) \propto T_c^{-1.2}, \ldots \Phi(^7Be) \propto T_c^{8}, \ldots \Phi(^8B) \propto T_c^{18} \qquad (3.14)$$

Note that the fluxes depend in different powers of the central temperature hence, when the data are fitted to T_c separately, the central temperatures thus obtained are inconsistent between different experiments. Also a little variation in Tc will cause an important variation of the fluxes. Diffusion mechanism are also considered to modify the abundances of the chemical elements hence the reaction rates and the neutrino fluxes[26]. Recent SSM consider Helium diffusion. However neutrinos deficit is still present.

CHAPTER 4:

SEASONAL EFFECT:

The solar magnetic field can be seen as the main superposition of a toroidal component and a poloidal one . A toroidal field is a field whose lines of force are circles around the solar axis, whereas a poloidal field is a field having its lines of force in the plane containing the solar axis. Each of the two components is antisymmetric with respect to the equatorial plane. It is this antisymmetry which plays a major role in the possibility of the observation of the seasonal effect. The origin of the presumed semiannual dependence is the combined effect of the inclination of the plane of the ecliptic with respect to the solar equator and the weakening of the solar magnetic field near the equator. When the Earth is near one of the intersection points of the Earth's orbit with the equatorial plane of the sun (at the beginning of June and the beginning of December), the production region of mainly the B^8 neutrinos is seen from the Earth through the equatorial slit in the magnetic field and the source of left-handed neutrinos is not weakened as a result of the leakage into right handed helicity state or into the antiparticle of any other flavor. On the other hand, when the Earth is maximally distant from the plane of the solar equator (at the beginning of September and the beginning of March) the neutrinos arriving to the Earth traverse a strong toroidal magnetic field and the detected flux should be minimal. Let us give a brief idea of the present understanding on the solar magnetic field. Because the sun is a gas, it can spin faster at the equator than at the poles, this effect is known as differential rotation. The sun has an electromagnetic dynamo in the convective zone, the convection and the differential rotation drive this dynamo to generate magnetic field lines east- west along the equator. It mixes up the polarities so that field reverses after 11 years end the cycle repeats after 22 years have elapsed. The main point here is that convection and differential rotation drive the solar dynamo and

produce the magnetic activity cycle. The turbulent motion of the conducting fluid generates and maintains a magnetic field on a large scale and produces a fluctuating component on a small scale [27]. Neutrinos while traveling through the convective zone will encounter each of the above components.

4.1: CALCULATING PROCEDURE:

Our thesis deals with the study of the effect of neutrino interaction with the sun's magnetic field on neutrinos fluxes.

Let us first emphasis on the experimental situation. The Homestake experiment detects neutrinos through the reaction: $^{37}Cl + \nu_e \rightarrow {}^{37}Ar + e^-$

which energy threshold is of 0.814 MeV. 14% of the neutrino that are detected are from the ^{7}Be reaction (E = 0.86 MeV), 78% are from the ^{8}B decay. The apparent time variation of the detection rate motivate the possible anticorrelation of neutrinos flux with the solar activity[28,29].

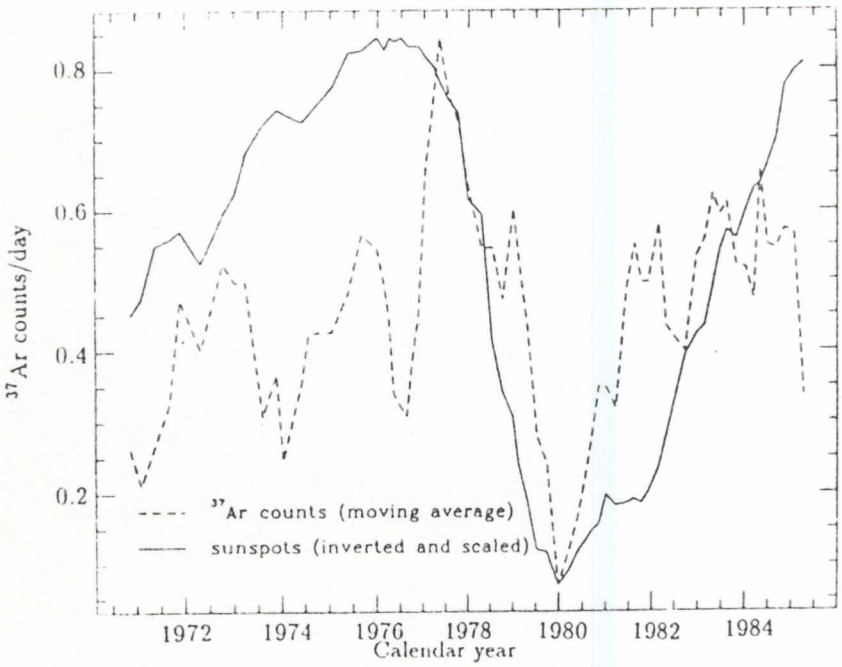

fig(4.1)

On the other hand, Kamiokande experiment which is sensitive to all of the neutrino flavor, detects exclusively high energy neutrinos coming from ^8B and didn't see any particular time variation of the flux. Gallium experiments observe the lowest energy neutrinos which are produced in the pp chain. Their energy ranges up to 0.42MeV. They account for 54% of the total flux, whereas the Be^7 and B^8 neutrinos account for 26% and 11% respectively. No time variation has been seen. Either this situation implies that the ^7Be neutrinos are more depleted than the ^8B ones or that the variation observed in Homestake is just a false effect. Gallex experiment has recently been calibrated, it results where consistent to 1.04 [30]. This scenario appears to be consistent with an energy dependence of the flux suppression. In fact, whereas the pp neutrinos are expected to be the least suppressed, ^7Be neutrinos undergo an important suppression at a rate which can be as large as 50%, in which case the ^8B neutrinos have to be the most suppressed. This is why the actual solar neutrinos problem is said to be that of the ^7Be neutrino deficit.

We consider Majorana neutrinos, and restrict ourselves to the two generation case.

The evolution of the state $\nu \equiv \left(\nu_e, \nu_\mu, \bar{\nu}_e, \bar{\nu}_\mu\right)$ through the Sun is:

$$i\frac{\partial \nu}{\partial t} = \begin{pmatrix} \frac{\Delta^2}{2E}\sin^2\theta + a_e(t) & \frac{\Delta^2}{4E}\sin 2\theta & 0 & \mu B \\ \frac{\Delta^2}{4E}\sin 2\theta & \frac{\Delta^2}{2E}\cos^2\theta + a_\mu(t) & \mu B & 0 \\ 0 & \mu B & \frac{\Delta^2}{2E}\sin^2\theta - a_e(t) & \frac{\Delta^2}{4E}\sin 2\theta \\ \mu B & 0 & \frac{\Delta^2}{4E}\sin 2\theta & \frac{\Delta^2}{2E}\cos^2\theta - a_\mu(t) \end{pmatrix} \nu \qquad (4.1.a)$$

where

$$\Delta^2 = m_2^2 - m_1^2$$

μ denotes for the transition magnetic moment of the neutrino,

θ for the mixing angle in vacuum

$$a_e(t) = \frac{G_F}{\sqrt{2}}(2n_e - n_n)$$

$$a_\mu(t) = -\frac{G_F}{\sqrt{2}} n_n$$

n_n and n_e are respectively the neutron and electron densities in the Sun

G_F is the Fermi constant.

We have considered the following electron and neutron densities in the Sun:

$$n_e(r) = 2.4\ 10^{26} \exp(-11.11\ r / R_S)$$
$$n_n(r) \approx \frac{n_e(r)}{6} \qquad (4.1.b)$$

In order to distinguish the spin matter resonance from the MSW one, we take the vacuum mixing angle equal to zero ($\theta = 0$). The system (4.2) decouples into two systems describing separately the evolution of $(\nu_e, \bar{\nu}_\mu)$ *and* $(\bar{\nu}_e, \nu_\mu)$.

Consider the following system:

$$i\frac{\partial}{\partial t}\begin{pmatrix} \nu_e \\ \bar{\nu}_\mu \end{pmatrix} = \begin{pmatrix} a_e(t) & \mu B \\ \mu B & \frac{\Delta m^2}{2E} - a_\mu(t) \end{pmatrix}\begin{pmatrix} \nu_e \\ \bar{\nu}_\mu \end{pmatrix} \qquad (4.2)$$

assuming that neutrinos travel through matter with the speed of light, $x \approx t$ (in natural units).

We are going to deduce the electron neutrino survival probability in three ways:

a/ We will first assume that the adiabatic conditions are fulfilled.

b/ We will consider a correction term describing the resonant zone where the adiabatic conditions are almost violated.

c/ We will finally perform a numerical resolution of (4.2)

In the adiabatic case, the variation of the spin-matter mixing angle θ_{SM} is so small, that the electron neutrino evolution can be deduced from that of the mass eigenstates. That is, if the neutrino starts in an eigenstate of the Hamiltonian it

will track that eigenstate, while the mixing angle changes due to change in matter density.

$$\begin{pmatrix} \nu_e \\ \overline{\nu}_\mu \end{pmatrix} = \begin{pmatrix} \cos\theta_{SM} & -\sin\theta_{SM} \\ \sin\theta_{SM} & \cos\theta_{SM} \end{pmatrix} \begin{pmatrix} \nu_1 \\ \nu_2 \end{pmatrix} \qquad (4.3.a)$$

$$P^{(ad)}_{\nu_e \to \nu_e} = \frac{1}{2}\left(1 + \cos 2\theta^{C}_{SM} \cos 2\theta^{edge}_{SM}\right)$$

where the indices "C" and "edge" denote for the core and the edge of the sun respectively while "ad" is for adiabatic conditions. The mixing angle is given by:

$$\cos 2\theta_{SM} = \frac{\frac{\Delta m^2}{2E} - (a_e(t) + a_\mu(t))}{\sqrt{\left(\frac{\Delta m^2}{2E} - (a_e(t) + a_\mu(t))\right)^2 + (2\mu B)^2}} \qquad (4.3.b)$$

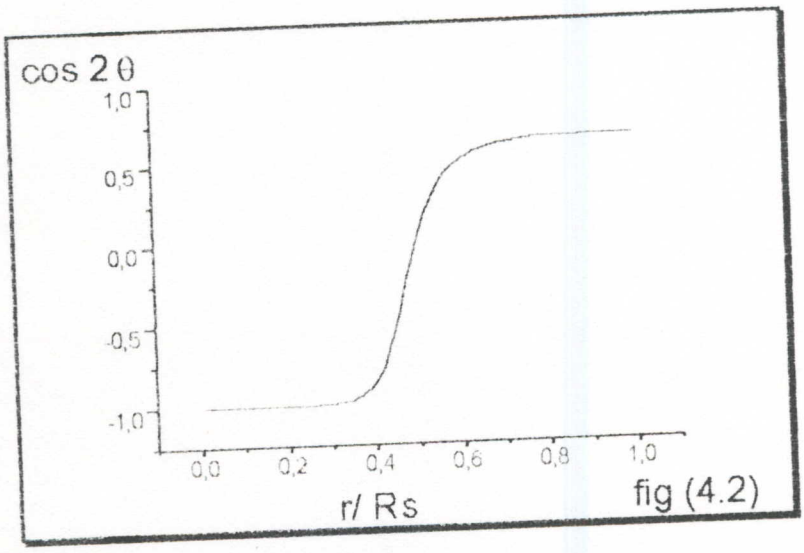

fig (4.2)

However it is at the resonance that the mixing angle undergoes a large variation . This is clearly shown on the graph fig (4.2) representing the variation of the mixing angle versus the solar radius. In conditions such those in the sun, where the density decreases exponentially, mixing angle would be subject

to an important rotation somewhere in the Sun i.e.: where the resonance condition is satisfied, that is, the diagonal elements of (4.2) become equal: $\frac{5\sqrt{2}}{6} G_F N_e = \frac{\Delta m^2}{2E}$ (4.4). Hence, we have to take into account the probability at the resonance. As we have seen earlier the general method for calculating such probability follows from Landau. We have noticed that because of the smallness of the width of the resonance ($\propto 2\mu B$), the corrections induced in the above method by the use of a linearly (P_{LZ}) or an exponentially (P_C) decreasing of the electron density are not significant. The following table shows the values of P_{LZ}, P_C and P_{num} for resonance occurring in the radiative and the convective zone of the sun for magnetic field configuration (c)shown below. The survival probability is given by equation (2.20), where P_R denotes either for P_{LZ} or P_C.

Table 6

$\Delta m^2/E$ (ev)	P_{LZ}^T	P_C^T	P_{num}
$5.\ 10^{-14}$	0.676	0.684	0.638
10^{-13}	0.755	0.758	0.726
10^{-12}	0.880	0.882	0.850

If the mass difference between the Hamiltonian eigenstates and the energy of the neutrinos that undergo resonance, are such that resonance occurs in the convective zone, possible correlation between the neutrino flux and the solar activity can be investigated.

The latitude variation of the magnetic field in the convective zone, together with an adequate neutrino magnetic moment are presumed to be at the origin of a possible seasonal effect. Unfortunately, very little is known about the structure of the solar magnetic field, so that one is forced to use various magnetic field configurations. In our calculations, we have assumed the transverse magnetic

field profile to consist of two separate spherical symmetric pieces: a nonuniform internal magnetic field with its scale defined by the parameter B_1 and a magnetic field in the convective zone characterized by the overall scale B_0 which can vary in time with changing solar activity. The effect its fluctuating component has not been taken into account. We have used the following configurations[29]:

$$B(x)=\begin{cases} B_1\left(\dfrac{0.2}{x+0.2}\right)^2 & 0\le x\le 0.65 \quad B_1=10^7\,G \\ B_0\left[1-\left(\dfrac{x-0.7}{0.3}\right)^2\right] & 0.65\le x\le 1 \quad B_0=10^5\,G \end{cases} \qquad (a)$$

$$B(x)=\begin{cases} B_1\left(\dfrac{0.2}{x+0.2}\right)^2 & 0\le x\le 0.65 \quad B_1=5\ 10^6\,G \\ B_0/\cosh\left[20(x-0.7)\right] & 0.65\le x\le 1 \quad B_0=10^4\,G \end{cases} \qquad (b)$$

$$B(x)=\begin{cases} B_1\left(\dfrac{0.1}{x+0.1}\right)^2 & 0\le x\le 0.7 \quad B_1=2\ \ 10^6\,G \\ \dfrac{B_0}{1+\exp\left[(x-0.95)/0.01\right]} & 0.7\le x\le 1 \quad B_0=3.125\ 10^4\,G \end{cases} \qquad (c)$$

(4.5)

configuration (a) gives a vanishing magnetic field at the surface. For a giving configuration and varying values of B_0, we have determined the domain of $(\Delta m^2,\mu)$that should reproduce the data. For the two extreme values of B_0 the lower value is taken at most to be 1/10 of the upper one. We have superposed the iso-survival probabilities contours, plotted on $(\Delta m^2,\mu)$ plane. The different values of B_0 should modulate the magnitude of the magnetic field to simulate a latitude dependence. For the lower value of B_0, describing the magnetic field near

the equatorial plane, the survival probability is higher and vise versa. In order to determine the maximum and the minimum fluxes with the corresponding uncertainties, we have proceeded to a statistical analysis of the experimental results, spread from 1970 to 1992 for Homestake experiment [31,32,33,34]. For the Gallex experiment, the data spread from 1989 to 1992. It is worthwhile to notice that the seasonal effect has ,if the correlation with the solar magnetic field is effective, to be superposed to the effect of the sunspots number.

We have considered a linear fit of the Ar rate, that is: $R_{ar} = a_S + b_S S$, corrected with the seasonal effect by the cosine function:

$$R_{ar} = a + b\,S\,z \tag{4.6}$$

where $z = \cos(2\pi (x-0.43))$

S denotes for the Sunspot number , x for the time in years ,0.43 corresponds to June.

We obtained the following results:

$$a = 0.2199 \pm 5.434\ 10^{-2}$$
$$b = (1.319 \pm 6.212)\ 10^{-4} \tag{4.6.a}$$

with $\chi^2 = 19.79$

For the Gallex detector, no time variation seems to be favored, the coefficients of the linear fit are the following:

$$a = (74.515 \pm 17.442)\ \text{(SNU)}$$
$$b = (-1.174 \pm 0.1988)\ \text{(SNU)} \tag{4.6.b}$$

with $\chi^2 = 10.13$

The absence of any published monthly collected data for Kamiokande experiment, makes the analysis of the seasonal effect for this experiment impossible. Hirata[35] shows that no seasonal effect is the Kamiokande experiment. One can only try to deduce the minimal value of the convective magnetic field which will cause a variation of 5% of the solar neutrino flux. Such observations should be available in the super Kamiokande.

For the plot of the iso-probability contours, we have used the expression (2.20) of the survival probability and Landau-Zener term for the resonant probability.

The iso-probability curves correspond to March and June rates of 1992, the experimentally available domain to the survival probability is the following:

$$R_{march} = 0.2199 \pm 5.434\ 10^{-2}$$
$$R_{june} = 0.228 \pm 0.094 \qquad (4.6.c)$$

We have finally performed a numerical resolution of (4.2) [36]. We have to solve a system of differential equations with the initial conditions: $\begin{pmatrix} \nu_e \\ \bar{\nu}_\mu \end{pmatrix} \equiv \begin{pmatrix} 1 \\ 0 \end{pmatrix}$.

This system is a good illustration of the importance of the calculation of the eigenvalues of the system before choosing any numerical method.

For any differential system $\Psi' = A\Psi$, the stiffens coefficient is defined by:

$$\eta = \frac{Max|\Re e\ \lambda_i|}{Min|\Re e\ \lambda_i|} \qquad (4.7)$$

where $\Re e(\lambda_i)$ denotes for the real part of the eigenvalue λ_i of A. This coefficient defines the stability of the system. Indeed when this ratio become important, the usual methods for solving differential systems based on Taylor expansion to

different orders (Euler, Runge-Kutta) will fail. They diverge, at once, or in the best cases enforce the use of small stepsize $\leq 10^{-6}$.In such cases, it is worthwhile either to use implicit methods or methods based on the following algorithm:

$$\Psi(x+\Delta x) = U^{-1}\, e^{-iD\,\Delta x}\, U\, \Psi(x) \tag{4.8}$$

where D is the eigenvalues matrix , U the diagonalization matrix. For a sufficiently small stepsize, each of the elements of U, U^{-1} and D matrices vary so slowly that the above approximation is meaningful. Decoupling the real part from the imaginary part in system (4.2) induce imaginary eigenvalues in the spectra of the decoupled system, such that it became unstable, and the usual methods are far from leading to the right results. In such cases we are forced to reduce the stepsize not to reach a better accuracy but to assure the convergence of the method. An implicit Kutta method in which the value of the unknown function at the present step (say : x + Δ x) enters together with its value at the last step could also be used:

$$\Psi\,(x+\Delta x) = f\,(\Psi\,(x+\Delta x),\, \Psi\,(x)) \tag{4.9}$$

Finally, we have proceeded to the calculation of the average of the survival probability over energy. For radiochemical detectors, one has to take into account the efficiency of extraction of the transformed atoms after the neutrino capture. For Kamiokande detector the average survival probability given by:

$$\overline{P} = \frac{\int_{E_0}^{E_1} \sigma\,(E)\;\varepsilon(E)\;\phi\;(E)\;P_{\nu_e\to\nu_e}(E)dE}{\int_{E_0}^{E_1} \sigma\,(E)\;\varepsilon\;(E)\;\phi\;(E)\;dE} \tag{4.10}$$

where σ(E) is the cross section for a given detector at energy E, ϕ is the

distribution in energy of the neutrinos produced in the decay of B^8, $\varepsilon(E)$ is the detector efficiency. For the product $\sigma(E)\,\varepsilon(E)\,\phi(E)$, we have fitted the curves given in [37]. Calculations will show even or not an average over energy is effective.

Table 7

$E/\Delta m^2$ (eV^{-1})	integrated probability	probability at an average energy
10^{13}	0.7217	0.726
2.10^{13}	0.6553	0.6381
10^{14}	0.1267	0.0801
10^{15}	0.4432	0.4455
10^{16}	0.5192	0.5192

The above calculations were obtained using configuration (4.13-c) of the magnetic field. Whenever very precise calculations are not needed, integration of the survival probability over energy can be skipped. Also the dispersion in the zone of production of neutrinos should be taken into account in the computation of the survival probability namely for the spread sources (like the pp one), see fig (3.2). The average probability is hence given by:

$$\overline{P} = \frac{\sum_i f_i \int_{E_0}^{E_1} \sigma(E)\,\varepsilon(E)\,\phi(E)\,P_{r_i \to 1}(E)\,dE}{\sum_i f_i \int_{E_0}^{E_1} \sigma(E)\,\varepsilon(E)\,\phi(E)} \qquad (4.11)$$

where r_i is the distance from the center, it is normalized with respect the the solar radius, $P_{ri\to 1}$ denoting the integrated survival probability from r_i to 1, f_i denoting the quantity of neutrinos produced in the volume delimited by r_i and $(r_i + dr)$ $(d(\text{Quantity})/d(R/R_S))$ in fig(3.2). In the case of the B^8 neutrinos for which we have performed such precise calculations no more accuracy has been noticed.

CHAPTER 5

RESULTS AND DISCUSSION:

Let us first focus on the statistical analysis we have performed. Our choice of the fit function was dictated by our aim to look for any seasonal effect embedded in the available data (4.6). Homestake experiment for which the analysis was done on 101 values allows us to determine the parameters defining the fit function. However, it seems that a more stringent analysis should be done. Indeed, by considering the maximal error in the collected data, our results are consistent to a confidence level of the order of 5%, one has to judge such procedure by performing an F test for example. No information could be extracted from the fit function related to Gallex data concerning the neutrinos parameters, the errors on the fit parameters being important compared to the parameters, although, the seasonal effect could be excluded with a confidence level of 75%. The recent published work of the Gallex group excluded any observed time variation with a confidence level of 82% [38].

This situation could be a guess of an energy dependence of the solution to the possible anti- correlation of the solar neutrino flux with the Sun activity. Indeed Gallex and Homestake experiments are concerned with different domains of neutrino energy spectra (fig 3.1). On the other hand, we have discussed earlier that it is at the resonance that the mixing angle undergoes an important variation (fig 4.2). From the resonant condition (4.4) it can be seen that it is the lower energy neutrinos which undergo resonance in deeper regions of the Sun rather than the high energy neutrinos. Taking these two remarks altogether, one can conclude that provided that Δm^2 is such that resonance for pp neutrinos (which are the ones mostly detected by Gallex) occurs in the radiative zone ($6.9\ 10^{-9} \leq \Delta m^2 \leq 1.6\ 10^{-5}$ (eV^2)) such a discrepancy could be explained.

We have solved the system of differential equation (4.2) first by assuming that the adiabatic conditions were fulfilled $\gamma >> 1$. Assuming a constant magnetic field of 2.10^6 G in the whole of the Sun, we plotted in fig (5.1.a) the analytical survival probability of an electron neutrino produced at the center of the Sun to emerge from its surface without changing its flavor in function of $E / \Delta m^2$. $E / \Delta m^2$ is an important parameter in locating the resonance region. Indeed for a resonance to occur anywhere in the Sun, $E / \Delta m^2$ should be bracketed between :

$2.10^{10} \leq \frac{E}{\Delta m^2} \leq 10^{15}$ (eV^{-1}). For a resonance to occur in the convective zone:

$2.10^{13} \leq \frac{E}{\Delta m^2} \leq 10^{15}$ (eV^{-1})

In a second step we have solved the system (4.2). The results are shown in fig(5.1.b) for a constant magnetic field and fig(5.2.b) for a space varying magnetic field by considering the configuration (4.5.c).

The numerically generated survival probability is well approximated by that generated analytically which follows from equation (2.20). However the situation is not very good when resonance occurs closely to the surface.

Let us give some comments on these figures.

When $\frac{\Delta m^2}{E}$ is comparable to μ B there will be an energy dependence of the mixing angle, (4.3.b) -the magnetic off-diagonal mixing terms become important- and a large depletion sets in. This defines two regions of maximal depletion in the case of differently defined magnetic field configuration in the radiative and convective (fig (5.2.a) and fig(5.2.b)), whereas only one region of depletion is observed in the case of a constant magnetic field (fig(5.1.a)- fig(5.1.b)).

As $\frac{\Delta m^2}{E}$ decreases further, the mixing angle become energy independent and hence the leaving off in each of the above figures. Therefore the probability at the edge of the Sun should depend on the magnetic field strength at the surface.

Since the strength of the magnetic field is not well known, we have tried to see the variation of the survival probability in terms of the overall scale of the magnetic field both in the radiative and the convective zones. Considering the configuration (4.5.c) of the magnetic field and assuming a resonance in the radiative (convective) zone by taking $\frac{\Delta m^2}{E} = 10^{-13}$ eV(10^{-14}eV), we plotted in fig (5.3.a) (fig(5.3.b)) the electron neutrino survival probability versus B_1 (B_0) . What one can learn from such curves is that for any anticorrelation with the solar magnetic field to be significant a magnetic field as high as 10^3 kG for B_1 and 6kG for B_0 is needed.

The main difficulty in the analysis of the seasonal effect is due to the inexistance of any latitude parametrization of the magnetic field. To overcome such a difficulty we have assumed that it latitude dependence could be represented by letting B_0 vary. For each of the configurations given in (4.5), we have plotted the isoprobability curves on (μ_ν ,Δ m^2) plane by taking for B_0 the half and the 1/10 the given values in (4.5). The maximal neutrino flux has been associated with these values. In each case we have determined the limits on μ_ν and Δ m^2 that should reproduce the rates for March and June 1992 given by the fit function.

$$R_{march} = (2.199 \pm 0.543)\ 10^{-1}$$

$$R_{june} = (2.28 \pm 0.94)\ 10^{-1}$$

The allowed domain for March rate is $0.17 \leq R_m \leq 0.274$ and for June rate it is bracketed $0.134 \leq R_{June} \leq 0.322$, see fig (5.4.a,b,c) ,fig (5.5.a,b,c) and fig (5.6.a,b,c).

The following table summarizes the limits obtained after the superposition of the iso-probability curves, where the allowed domain for the plot corresponding to the full value of B_0 (when the Earth is at maximum latitude) is given by the limits on March rate, whereas that corresponding to the reduced values of B_0

(when the Earth is near the equatorial plane) is given by the limits on June rate. The superposition of the two domains gives the limits on the neutrino parameters, the results are summarized in the following table.

Table7

magnetic field configurations	μ_ν (in μ_B units)	$\Delta m^2(eV^2)$
config(4.5a), $_{1/2}B_0$	$7.\ 10^{-12}$	$1.7\ 10^{-9}$
$_{1/10}B_0$	$3.8\ 10^{-11}$	$1.7.10^{-9}$
config(4.5b), $_{1/2}B_0$	$1.9\ 10^{-10}$	$4.5\ 10^{-9}$
$_{1/10}B_0$	$2.8\ 10^{-10}$	$4.8\ 10^{-9}$
config(4.5c), $_{1/2}B_0$	$2.1\ 10^{-11}$	$1.9\ 10^{-9}$
$_{1/10}B_0$	$1.1\ 10^{-10}$	$2.\ 10^{-9}$

The limits on μ_ν indicate again that we have to look beyond the SM to explain the neutrinos properties, namely seek models which allow one loop contribution to the magnetic moment to be of the order of 10^{-11} μ_B that is some 10^8 time the typical radiative mass in the minimally extended SM. Furthermore, it is thus clear that only models of neutrinos which allows highly degenerate masses are required in order to explain the solar neutrino deficit. This could come from models which implement the sea saw mechanism (1.26) and thus have a second energy scale higher than the electro-weak scale, or alternatively from models which make use of pseudo-Dirac neutrinos (Majorana mass terms much smaller than Dirac mass term).

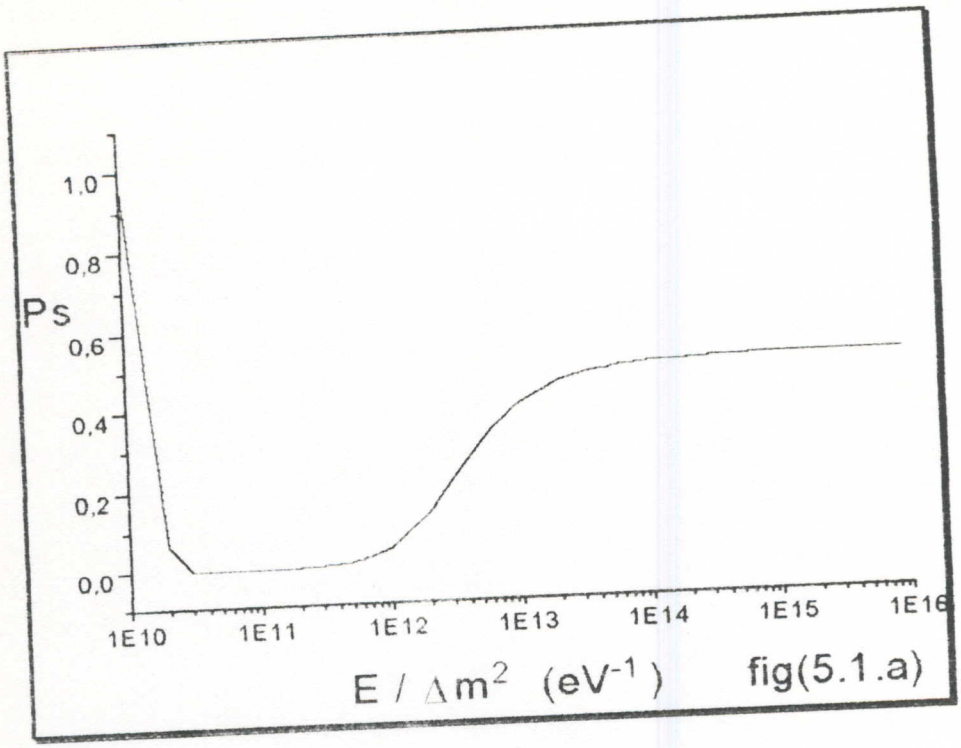

fig(5.1.a)

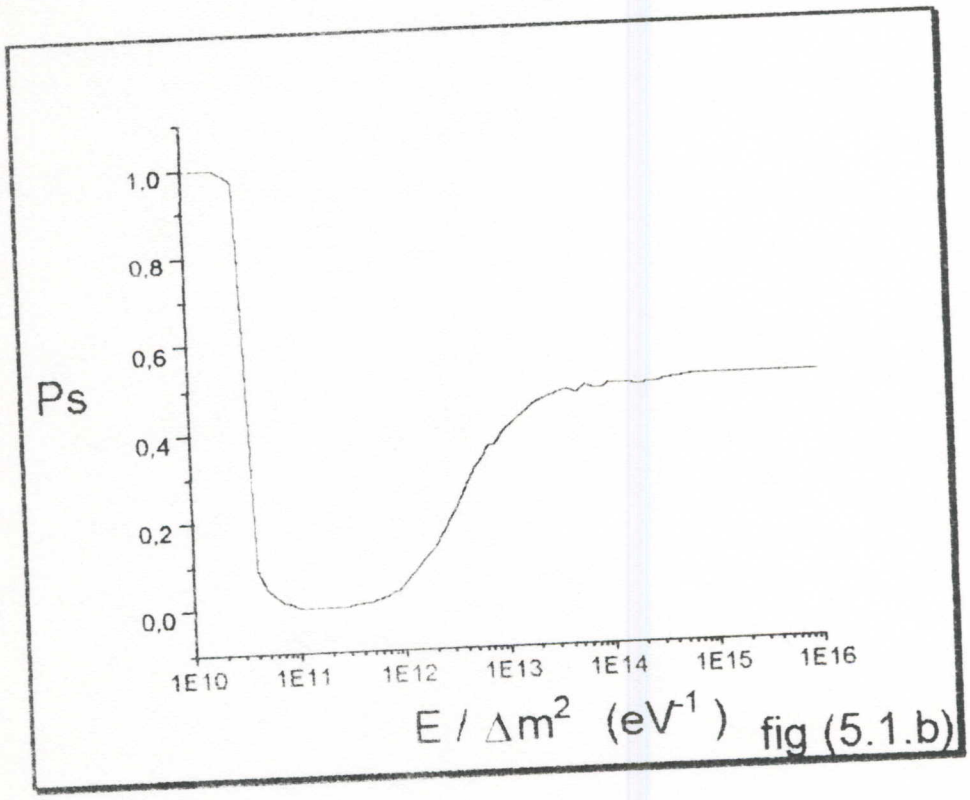

fig (5.1.b)

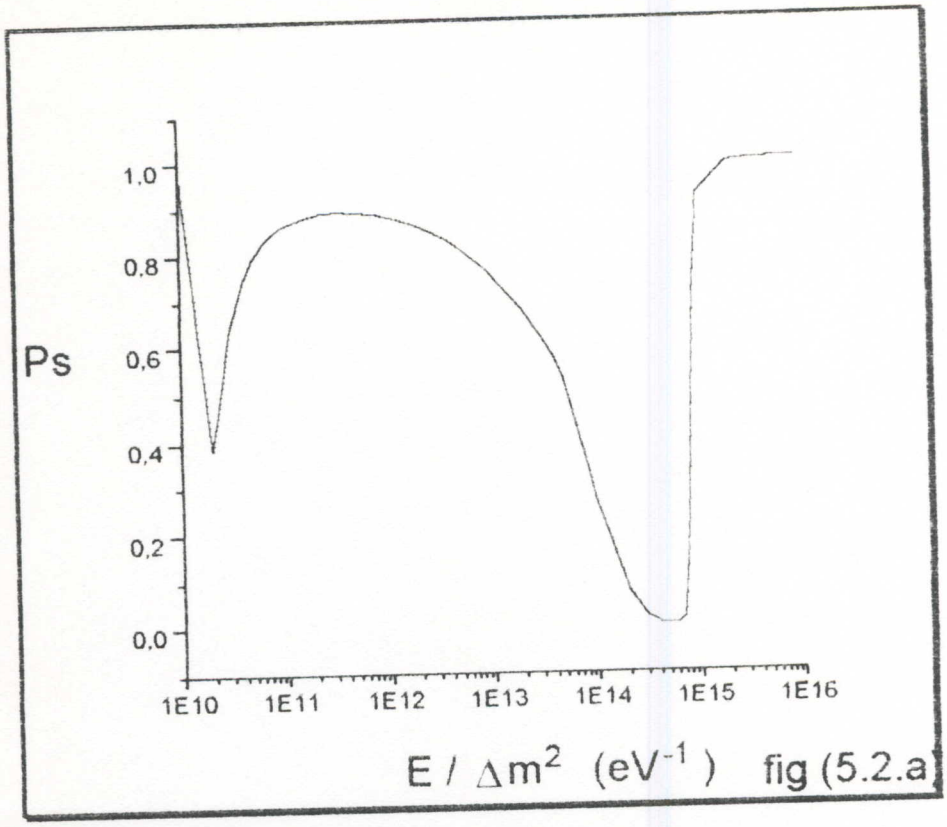

fig (5.2.a)

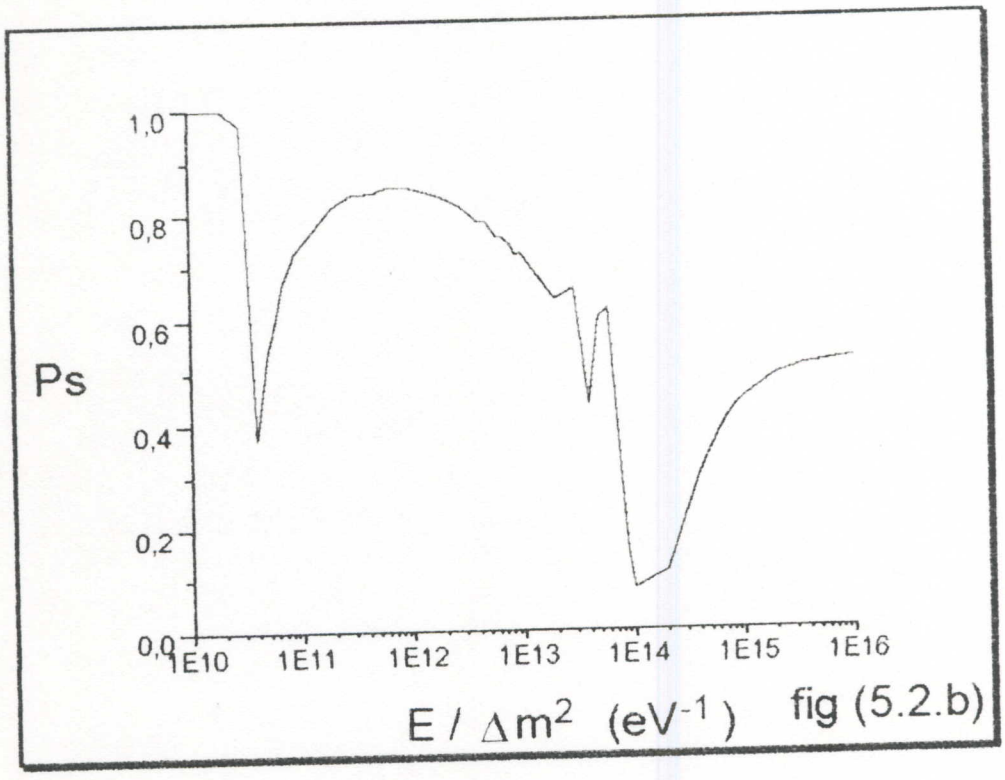

fig (5.2.b)

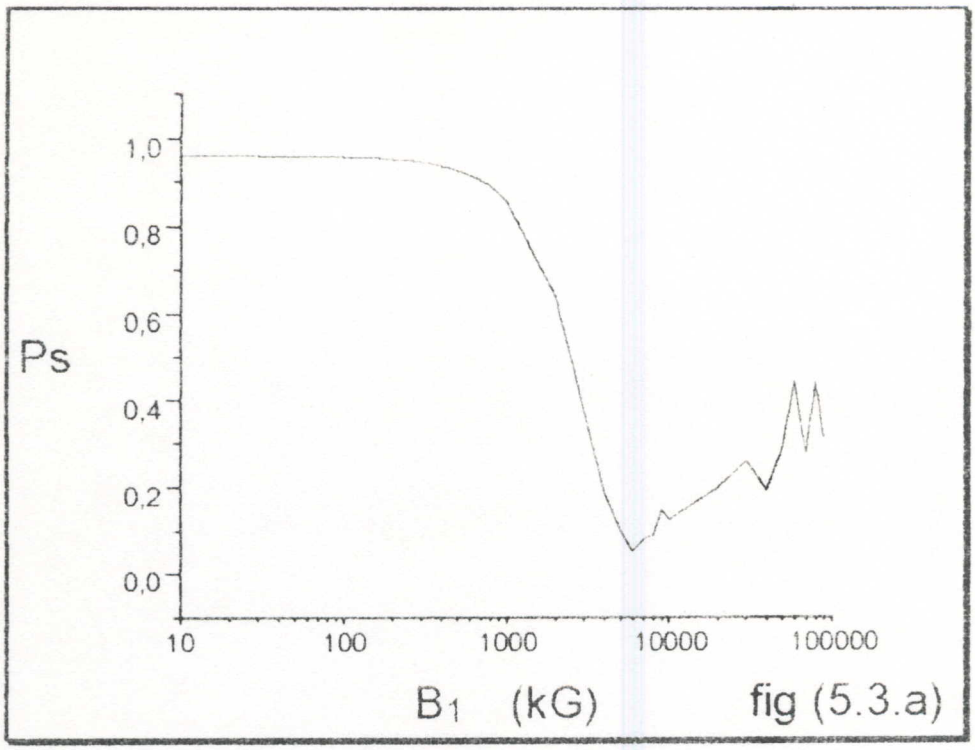

fig (5.3.a)

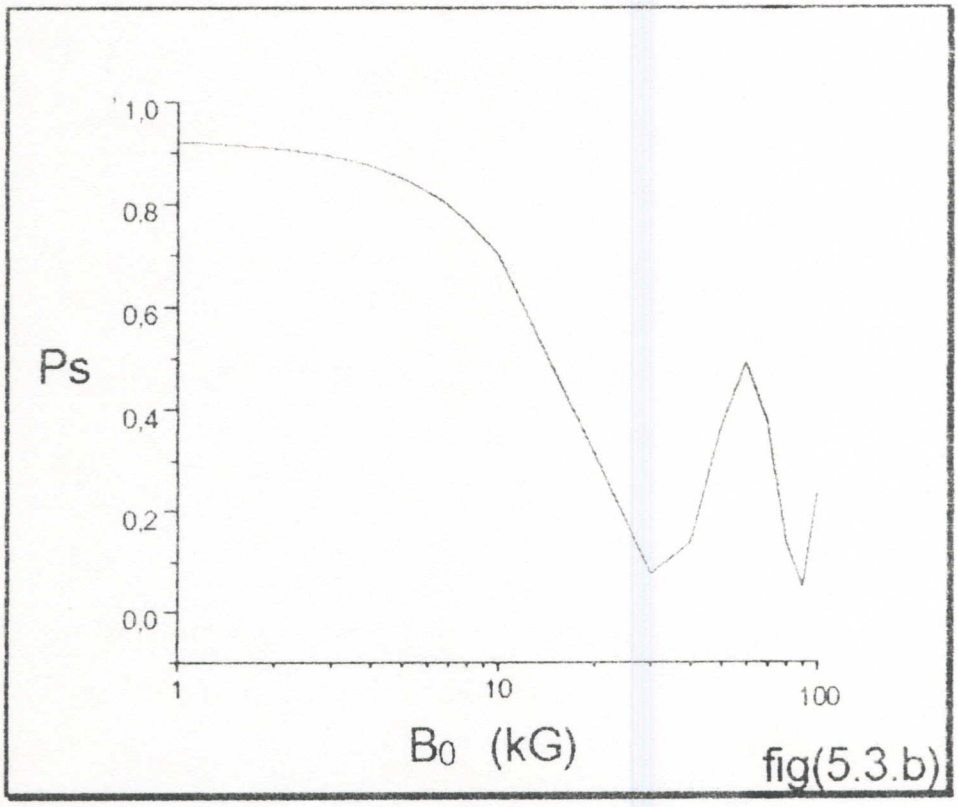

fig(5.3.b)

fig(5.4.a) B0=3.125e4

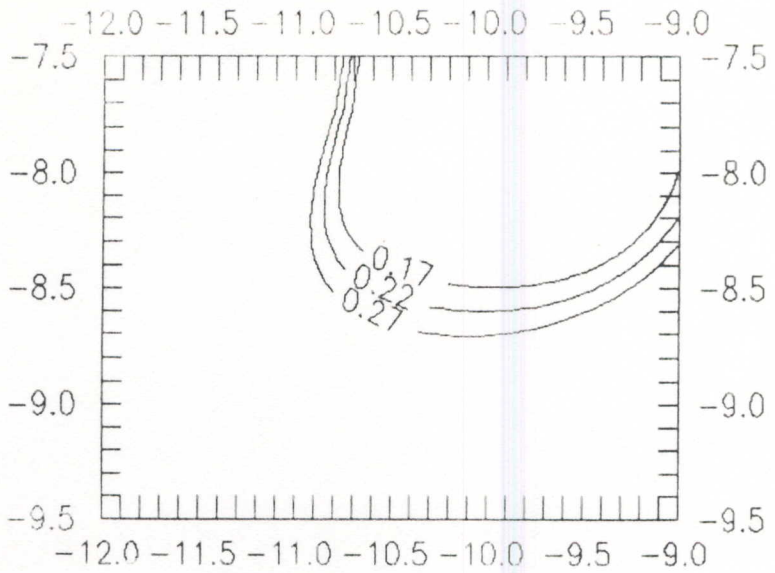

fig(5.5.a) B0=1e4

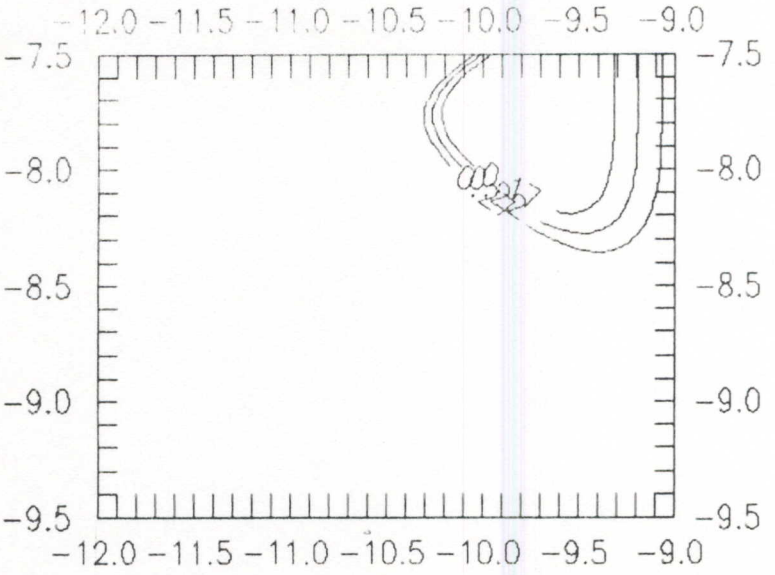

fig(5.6.a) B0=1e5

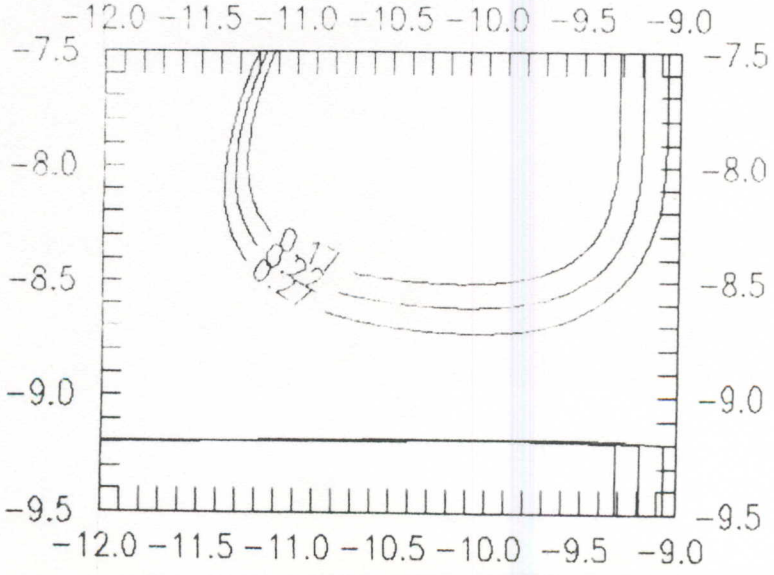

fig(5.4.b) B0=1.562e4

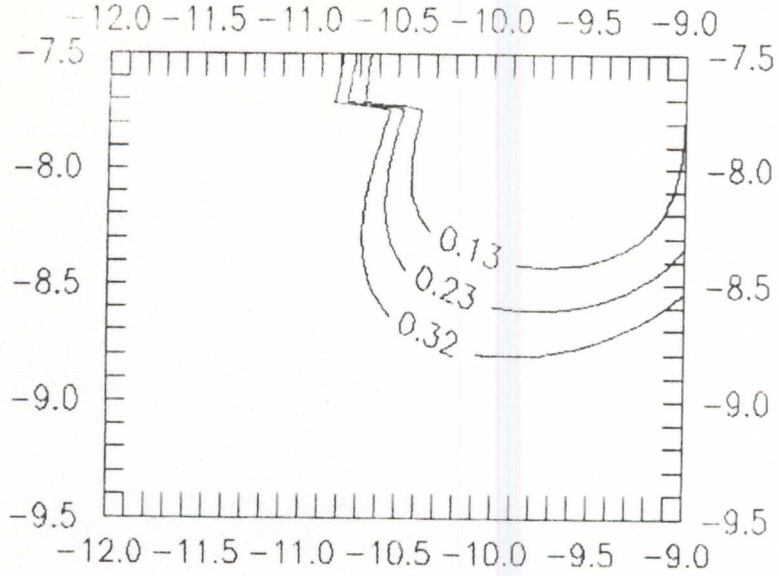

fig(5.5.b) B0=5e3

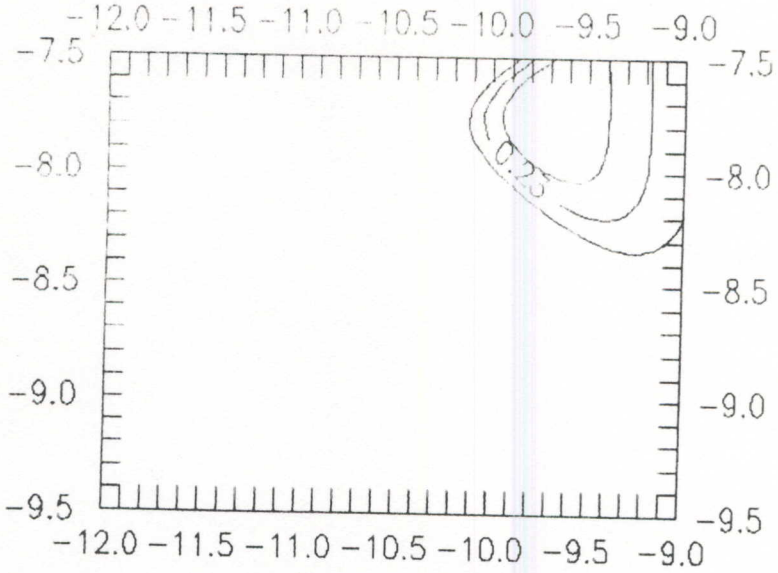

fig(5.6.b) B0=5e4

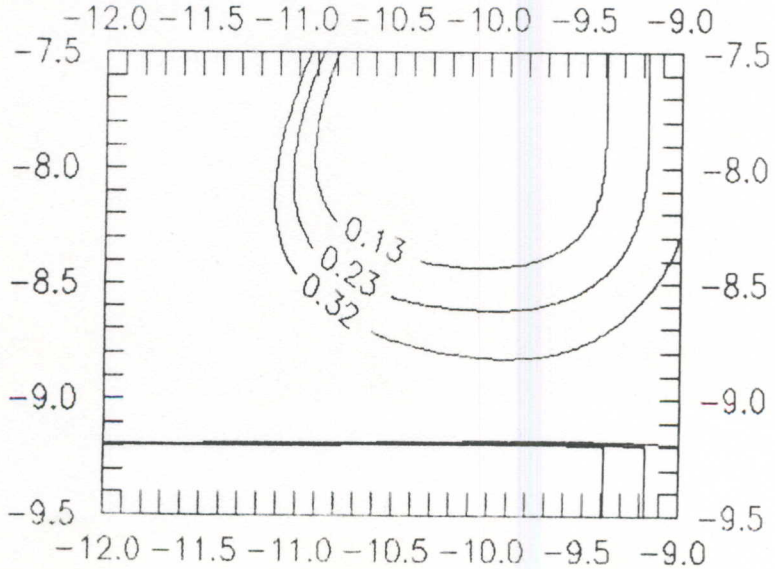

fig(5.4.c) B0=3.125e3

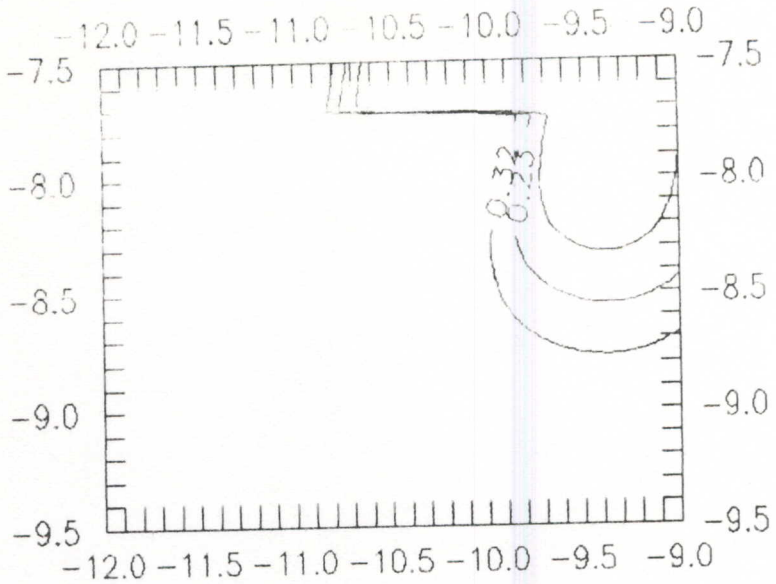

fig(5.5.c) B0=1e3

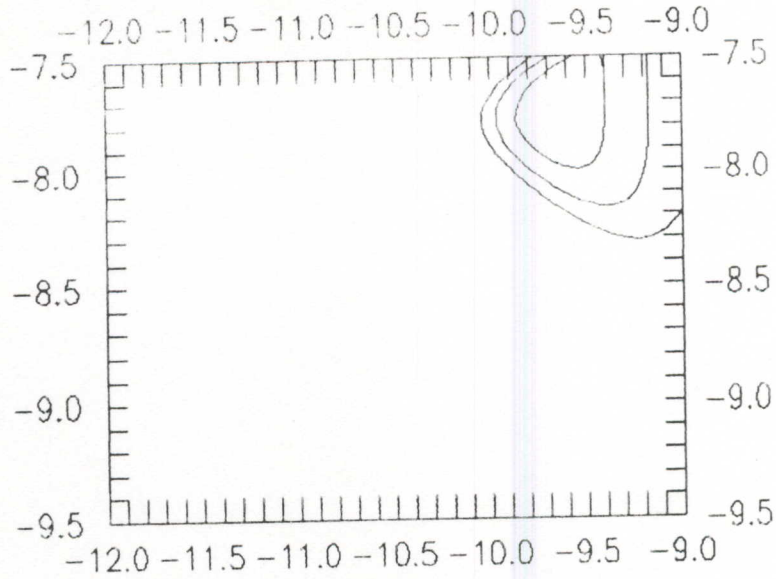

fig(5.6.c) B0=1e4

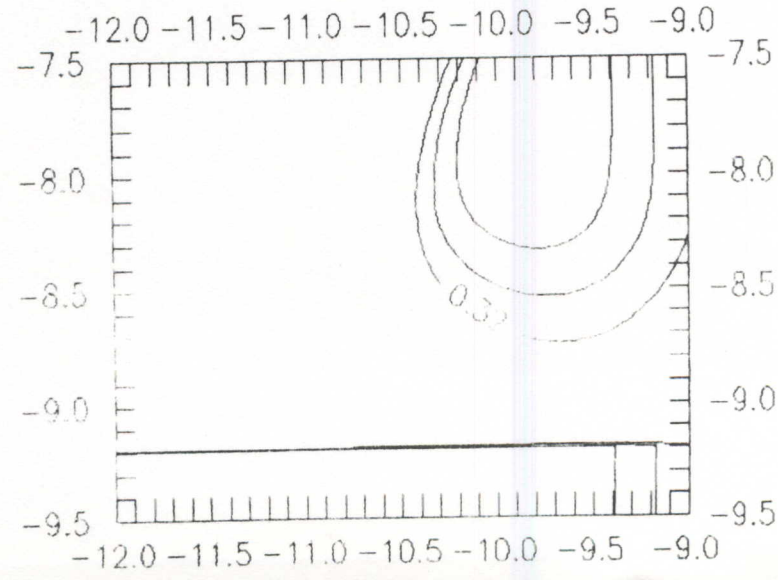

CONCLUSIONS:

The statistical analysis we have performed enabled us to make it plausible that a time variation of the neutrinos flux do exist in the Homestake data, whereas no time variation has been found with the Gallex data. However the treatment of the uncertainties should be more stringent.

For the survival probability to be reduced by the allowed experimental rate (1/3, 1/2), the overall factor of the magnetic field in the radiative (convective) zoneB_1 (B_0) should be bigger than 10^3 kG (6 kG). More precise calculations should be done by performing numerical computations with exact distribution density of electrons [23] and a functional dependence of the magnetic field with latitude. The sensitivity of the solution to a fitted density is important near the surface.

We note that a more complete analysis is needed which would take into account the MSW effect, in particular for the equatorial plane where the toroidal magnetic field is vanishingly small, so that the deficit could be shaded by both the MSW and the spin flavor precession .

We do mention again that a fluctuating magnetic field is supposed to exist in addition to the mean field, the only one we have considered in our calculations, and that it could play a role in explaining part of the flux deficit.

In the limits of our calculations, the lowest limits of Δm^2 and μ_ν we could obtain are given in table 7. Physics beyond the minimally extended SM should be invoked.

Let us recall that a deficit is noticed on the neutrino fluxes from different sources (sun, atmosphere) and hence of different energies, an accumulation of data is needed to conclude about the origin of the deficit. Clearly, the solution to the solar neutrino problem lays with the data from future experiments which are planned to be high accuracy statistics (3000events/ year) with real time event detector capability. Some of them will offer the possibility of measuring the neutrino energy spectra, which is by far the most crucial test of whether the solution of the neutrino problem is an astrophysical one or a particle physics one.

NEUTRINOS DETECTORS:

Neutrinos constitute an important way of probing solar interior. In fact since the first results of Homestake experiments, many projects have been investigated. Some experiments are working at this time, others will take their first data in the near future. The table below summarizes the main characteristics of the operating detectors and the funded ones[39] .

Neutrinos are either produced by β disintegration or an electron absorption by the nucleus. They are detected via the following processes:

Absorption: The neutrino is absorbed by the target (A, Z) through the scheme:

$\nu_e + (A, Z) \longrightarrow e^- + (A, Z+1)$ exchange of the W^+ boson

This is the basis of the radiochemical detectors. They are sensitive only to the electron neutrinos. The transformed nucleus are extracted, thus no information on neutrino direction nor on it energy are collected.

Collision: - on heavy nucleus:

$\nu_x + (A, Z) \longrightarrow \nu_x + (A, Z)^*$ exchange of the boson Z

all neutrinos flavor can therefore be detected.

- on electrons:

$\nu_x + e^- \longrightarrow \nu_x + e^-$ exchange of the bosons Z, $W^{\pm}$

The characteristics of the recoiled electrons are correlated to those of the incident neutrinos. The detectors based on such processes can particularly identify the background.

Homestake experiment:

It is a radiochemical detector, constituted of an immense volume of 615 tons of perchloretylene C_2Cl_4 in the Homestake mine. This huge volume had been chosen because of the smallness of the cross section of interaction of neutrinos, of the order of 10^{-41} cm^2 for an energy of 14 MeV.

The reaction follows the scheme:

$$\nu_e + {}^{37}Cl \longrightarrow e^- + {}^{37}Ar$$

After a certain time of exposure the argon is extracted. First of all, 1 cm^3 of non radioactive ^{36}Ar or ^{38}Ar is injected in the C_2Cl_4. It injection will lead to the determination of the efficiency of the extraction of argon. Indeed, the injected quantity is compared to the recoiled one. The time of exposure is about of 2 months.

Kamiokande experiment:

It is based on the following reaction of collision:

$$\nu_x + e^- \longrightarrow \nu_x + e^-$$

The target is a cylindrical volume of 16 m height and 15.6 m of diameter of pure water. The electron energy is correlated to the direction of the incident neutrinos. This experiment provided a particular proof of the solar origin of the detected neutrinos. The efficiency of detection is of 50% (90%) for an energy of 5.2 (6.7) MeV. The background is essentially due to gamma rays and also to the reactions induced by the cosmic muons. However, they are absorbed by the pure water. The fiducial volume is hence reduced to 680 tons.

Gallium experiment:

The importance of the radiochemical detectors is in the possibility of detecting the less energetic neutrinos. This property depends on the energy threshold of the basic reaction.

The reaction : $\nu_e + {}^{71}Ga \longrightarrow e^- + {}^{71}Ge$, has an energy threshold of 233 keV, thus offering the possibility of detecting the most abundant pp neutrinos of

maximal energy of 420 keV. The SSM predictions for the gallium detector span a relatively narrow range varying from 113 SNU[40] to 122.5 ± 14 SNU (2σ) [41] , to 131.5 ±14 SNU (2σ) [42].

Two Gallium experiment are taking data. One is based on a target of a solution of Ga Cl_3 it is the Gallex experiment in Gran Sasso in Italy, the other, the SAGE experiment in Russia, has a solid target of gallium metal.

Gallex:

The exposure time is of 3 weeks. A volume of about 150 m^3/h is injected in the solution of Ga Cl_3 during 20 hours to extract the germanium atoms. The efficiency of extraction is estimates to be of about 95% , that of counting is of 65 %. The background is essentially due to the reaction ^{71}Ga (p,n) ^{71}Ge, it is estimated to 4 SUN. The first results from May 1991 to April 1992 give a mean flux of 83 ±19 (state) ± 8 (sys). These results confirm for the first time the detection of the pp neutrinos. A recent calibration of Gallex detector confirm the solar neutrinos problem. By using a radioactive source of Cr, and measuring the neutrinos thus emitted, the Gallex results are indeed fiable. The neutrino rate measured is (77.1±19) SNU [37], a deficit in the solar neutrino rate is still present. The experiment will probably be stopped on 1997.

SAGE:

The target is a volume of 60 tons of metallic gallium in reactors each of 7 tons. The operation of extraction of germanium is more complex than in the case of liquid target. The efficiency is of 80%. The background is reduced to 0.5 SNU.

FUTURE DETECTORS:

Sudbury Neutrino Observatory (SNO)

It uses 1 kton of heavy water D_2O. It detects neutrinos through the following reactions:

$\nu_e + d \longrightarrow p + p + e^-$ exchange a charged boson

measures the flux of ν_e

$\nu + e^- \longrightarrow \nu + e^-$ exchange neutral or charged bosons
measures each of the neutrinos flavors

$\nu + d \longrightarrow \nu + p + n$ exchange of neutral boson

The comparison of the different detected rates is a test of the effectiveness of the flavor oscillation. A measure of the neutrino spectra of energy is also foreseen. Such precise measure will approve or disapprove the particle physics solution of the solar neutrino deficit. Indeed , as it has been seen earlier , NSSM should not affect the shape of the neutrinos spectra from that predicted by the SSM.

Borexino (first step of Borex):

It observes essentially the ^{7}Be neutrinos. In a scintillate liquid, the recoiled electrons are detected in coincidence with gamma rays. This detector will be able to measure the neutrino flux at a given energy above 5 MeV . More restrictions should be available on neutrinos parameters.

From an other side, the observation of anti-neutrinos provides tests on the nature of the neutrino (Majorana or Dirac particle). The interesting reactions are the following:

$\bar{\nu}_e + d \longrightarrow e^+ + n + n$

$\bar{\nu}_e + p \longrightarrow e^+ + n$

Icarus:

It is a radiochemical detector, analogue to the chlorine one .

$\nu_e + {}^{127}I \longrightarrow e^- + {}^{127}Xe$ $\quad E_{th} = 0.789$ MeV

The cross section of capture of neutrinos by the iodine is higher than that corresponding to the chlorine. Hence , the event rate is much higher. This detector will verify the Homestake results.

SuperKamiokande:

It is an other new detector with a considerable improvements compared to the Kamiokande detector (which will work separately to S-K). It energy threshold is 5 MeV. It fiducial volume is 22000 tons of pure water. The events rate has been estimated to 50 neutrinos /day.

The future generation of detectors will certainly be able to verify many of the proposed solutions. The number of events will be considerably multiplied. The time variation will be eventually tested.

Table 9

	SITE	Fiducial Mass (tons)	Process	E_{th} (e) (MeV)	E_{th} (ν) (MeV)	Rate (Day^{1})	Background (Day^{-1})	Status
Homestake	USA (S. Dakota)	140 615t / C_2Cl_4	$^{37}Cl(\nu_e,e)^{37}Ar$	–	0.814	0.3	0.08	taking data
SAGE	Russia Baksan	60t Ga metallic phase	$^{71}Ga(\nu_e,e)^{71}Ge$	–	0.233	0.75 1.5	0.06 0.12	taking data
Gallex	Italy Gran Sasso	30.3 $GaCl_3$+HCl	$^{71}Ga(\nu_e,e^-)^{71}Ge$	–	0.233	0.75	0.06	taking data
Kamiokande	Japan	680 water	$\nu_x+e^-\rightarrow\nu_x+e^-$	7.5	≈ 8.5	.3	.5	taking data
Super-Kamiokande	Japan	22000 water	$\nu_x+e^-\rightarrow\nu_x+e^-$	5	6	23	6.6	starting in 96
Sudbury neutrino obser-vatory(SNO)	Canada	1000 d_2O NaCl	$\nu_e+d\rightarrow p+p+e^-$ $\nu_x+e^-\rightarrow\nu_x+e^-$ $\nu_x+d\rightarrow\nu_x+p+n$	5 5 5	6.4 ≈ 6 2.2	27 3 7.5	3 3 2.5	starting in 96
Icarus	Italy Gran Sasso	3 x 5000 Liquid argon	$\nu_x+e^-\rightarrow\nu_x+e^-$ $^{40}Ar(\nu_e,e)^{40}K$	5 5	6 10	3 x 8 3 x 6.5	< 0.4	starting in 98
Hellaz	Italy Gran Sasso	12 Helium	$\nu_x+e^-\rightarrow\nu_x+e^-$	0.1	0.22	15	10 - 100	proporsal
Borexino	Italy Gran Sasso	100 Trimethylbo-rate	$^{11}B(\nu_e,e^-)^{11}C$ $\nu_x+e^-\rightarrow\nu_x+e^-$	.25 - .7 2.0	≈ 0.41	50 ?	18 - 117	conditionally approved 96

Index of tables :

Index of figures:

REFERENCES:

[1] CERN courier , Vol 33, Nov. 1993.

[2] R.N.Mohapatra & P.Pal 1991 Massive Neutrinos in Physics and Astrophysics (World Scientific, Singapore).

[3] J. Bahcall International Symposium on Neutrino Astrophysics, Takayama/ Kamioka 10/92.

[4] J.Bahcall , Neutrino Astrophysics, Cambridge University Press, Cambridge, England, 1989.

[5] L.Wolfenstein, Phys .Rev. D17 (1978) 2369.

[6] S.P.Mikheyev & Yu.Smirnov, Sov.J.Nucl.Phys. 42 (1985) 913.

[7]M.B. Voloshin & M.I. Vysotskii Sov.J.Nucl.Phys 44 (3) Sept 86.

[8]M.B. Voloshin, M.I. Vysotskii & L.B.Okun Sov.J.Nucl.Phys 44 (3) Sept 86.

[9]Chong-Sa Lim , W.J.Marciano Phys.Rev.D 15 March 1988.

[10]E.Kh.Akhmedov, Phys.lett B213 (1988) 64.

[11] F.Halzen & A.D.Martin, Quarks & Leptons: An Introductory Course in Modern Particle Physics edited by J.Wiley & Sons.

[12] K.V.L.Sarma TIFR / TH / 94-13 PUB , Oct 94.

[13] S.K.Bilenky, S.T Petcov Rev. Mod. Phys , Vol 59, Num. 3,July 1987.

[14] B.Kayser with F.Gibrat-Debu & F. Perrier : The Physics of Massive Neutrinos Published by: World Scientific, Singapore, Lecture Notes in Physics Vol. 25 1989.

[15] C.W.Kim, A.Pevsner Neutrino Physics, Contemporary Concepts in Physics: Neutrino in Physics & Astrophysics.

[16] R.Peccei The Physics of Neutrino , Lectures presented at the Flavor Symposium, Pekin University, Beijing, Peoples Republic of China , Aug.1988.

[17] Palash B.Pal International Journal of Mod Phys. A. Nov 1991.

[18] T.K.Kuo , Phys. Reports 242 1994, 363-370.

[19] L.Landau, Mecanique Quantique, edition Mir.

[20] J. Pulido Phys. Reports , 211 , Num 4, 1992.

[21] D.D.Clayton 1983 Principles of Stellar Evolution and Nucleosynthesis, The University of Chicago Press.

[22] S.Turck-Chièze, W.Dappen, E.Fossat, J.Provost, E.Schatzman and D.Vignaud Phys.Reports, Vol 230 Num 2-4 Aug 1993.

[23] J. Bahcall & R. Ulrich, Rev.Mod.Phys, 60, 297 1988.

[24] F.J.Rogers & C.A.Iglesias , ApJ Sup 79, 507-568, April 1992.

[25] D.R.O.Morrison CERN-PPE /91-104 28 June 1991.

[26] E.Schatzman Ecole Juliot-Curie de Physique Nucleaire 1990.

[27] A.Nicolaidis , Phys.Lett.B, June 1991.

[28] K.S Babu, Rabinda N. Mohapatra, I.Z Rothstein , Phys. Rev. D Vol 44, Num 8,15 Oct 1991.

[29] E.Kh. Akhmedov, A.Lanza, S.T Petcov, report SISSA 169/ 94/ A-EP

[30] D.Vignaud Talk given at the Fourth School on Non Accelerator Particle Astrophysics ICTP, (July 1995).

[31] R.Davis , 1994, Prog.Part.Nucl.Phys, edited by: A.Faeshler, Pergamon Press, 32, 13-32.

[32] Anselmann et al, Phys.Lett. B283, 376,390,327 & 377.

[33] J.W.Bieber, D.Seckel, T.Stanev, G.Steigman, Nature 348 (1990) 407.

[34] T.Stanev, Talk given at the Int.Workshop "Solar Neutrino Problem: Astrophysics or Oscillation?" Gran Sasso, Italy, Feb 28- March 1, 1994.

[35] K.S.Hirata et al., Phys.Rev.Lett. 66 (1991) 9.

[36] W.H.Press et al., Numerical recipes , Cambridge University Press , New York 1986.

[37] V.Barger, R.J.N.Phillips, K.Whisnant Phy Rev D43 (1991)

[38] Gallex collaboration submitted to Phys.lett.B June 1995.

[39] J.P. Revol CERN - PPE / 93-84 27 May 1993.

[40] A.Dar & G.Shaviv, Preprint Technion Ph-94-5; G. Shaviv, Nucl.Phys.B (Proc.Suppl.) 38 (1995) 81.

[41] S.Turck-Chièze & I.Lopes, Ap.J.408 (1993) 347.

[42] J.N.Bahcall & M.H.Pinsonneault, Rev.Mod.Phys. 64 (1992) 885.